How much water vapour does the Tibetan Plateau release into the atmosphere?

Chaolei Zheng[1], Li Jia[1], Guangcheng Hu [1], Massimo Menenti[1, 2], Joris Timmermans[2]

[1] ~~State~~ Key Laboratory of Remote Sensing ~~Science~~and Digital Earth, Aerospace Information Research Institute, Chinese Academy of Sciences, Beijing 100101, China

[2] Faculty of Civil Engineering and Geosciences, Delft University of Technology, Delft, the Netherlands

Correspondence to: Chaolei Zheng (zhengcl@aircas.ac.cn)

带格式的: 上标

Abstract. ~~Evapotranspiration (ET)~~Water vapour flux, expressed as evapotranspiration (ET), is critical for understanding the earth climate system and the complex heat/water exchange mechanisms between the land surface and the atmosphere in the high-altitude Tibetan Plateau (TP) region. However, the performance of ET products over the TP has not been adequately assessed, and there is still ~~significant~~considerable uncertainty ~~regarding the amount of~~ in the magnitude and spatial variability in the water vapour released ~~by~~from the TP into the atmosphere~~, as well as its variation.~~. In this study, we evaluated 22 ET products ~~over~~in the TP ~~by validating with the~~against *in-situ* observations and basin-scale water balance estimations. This study also ~~inter-compared their~~evaluated the spatiotemporal ~~variations and~~ variability of the total vapour flux and of its components to clarify the ~~ET~~vapour flux magnitude and variability in the TP. The results showed that the remote sensing high-resolution global ET data from ETMonitor and PMLV2 ~~demonstrated~~had a high accuracy ~~comparable to the regional MOD16STM ET product~~, with overall better accuracy than other global and regional ET data with fine spatial resolution (~1km), when comparing with *in-situ* ~~observation. Their accuracy was also presented when~~observations. When compared with ~~the~~ water balance-~~based~~ estimates of ET at the basin scale, ~~which further indicated the overall accuracy of~~ ETMonitor and PMLV2 at finer spatial resolution and GLEAM and TerraClimate ~~for~~at the coarse- spatial resolution ~~ET products~~showed good agreement. Different products showed different patterns of spatiotemporal ~~variation patterns~~variability, with large ~~discrepancy occurring~~differences in the ~~middle~~central to western TP. The ~~multiple~~multi-year ~~averaged~~and multi-product mean ET ~~over~~in the TP ~~by these products was found to have an average value (~~was 333.1 mm/yr with a standard deviation~~)~~ of ~~350.34 (42.46)~~38.3 mm/yr. The ~~different~~ET components (i.e., plant transpiration, soil evaporation, canopy rainfall interception evaporation, open water evaporation, and snow/ice sublimation) available from some products were also compared, and the ~~separate~~ contribution of these components to total ET varied ~~substantially~~considerably even in cases ~~in which~~where the total ET ~~agrees by~~from different products~~. The response~~ was similar. Soil evaporation accounts for most of ~~annual ET to total precipitation, net radiation~~the total ET in the TP, followed by plant transpiration and ~~leaf area index was explored to present their governing effect on ET,~~canopy rainfall interception evaporation, while the contributions from open water evaporation and ~~the results indicated that precipitation effect mostly in the middle and northern TP and net radiation play significant role in the eastern TP~~snow/ice sublimation cannot be negligible.

带格式的: 字体: 倾斜

带格式的: 字体: 倾斜

1 Introduction

The Tibetan Plateau (TP) is also known as the ~~"~~‘Water Tower of Asia~~"~~’ as it is the source of 10 major ~~river basins~~rivers. Significant changes ~~have occurred~~ in the natural and social environments of the TP have occurred over the past 50 years (e.g., temperatures ~~warming~~have warmed twice as much as the global average over the same period), ~~providing a significant~~and there is considerable uncertainty ~~of~~about further environmental change (Immerzeel et al., 2020; Yang et al., 2014; Chen et al., 2015). Observations have shown significant changes in the environment, such as increased precipitation, decreased wind speed and snow days, ~~increasing at~~ increased surface solar ~~irradiance~~radiation, thawing of permafrost, melting of glaciers and snow, and greening of vegetation (Yao et al., 2012; Yang et al., 2014; Kuang and Jiao et al., 2016; Bibi et al., 2018; Z. Wang et al., 2018). These changes have ~~had~~ significant impacts on human living ~~environment~~conditions, as well as economic and social development (Wei et al., 2022; Yang et al., 2022). The TP can also affect the atmospheric circulation by altering the release of sensible and latent heat, which has a significant ~~impact~~implication on the climate in China, Asia, and globally (Wu et al., 2016).

~~Studying~~Water vapour flux, expressed as evapotranspiration (ET~~) over the Tibetan Plateau (TP)~~), is critical for understanding the earth climate system and the ~~complex~~com-plex heat/water exchange mechanisms between the land surface and the atmos-phere in the high-altitude TP region (Shen et al., 2015; Yang et al., 2023). ~~ET plays a crucial role in linking the water and energy cycles in the hydrosphere, atmosphere, soil and biosphere.~~ It is important as a covariate of the water and heat fluxes in the soil-vegetation-atmosphere system in the TP and as an indicator of climate and land surface changes (Sun et al., 2023; Yang et al~~.~~., 2023; Zhang et al., 2010). ~~It is expected that~~The TP is experiencing faster water phase ~~transformation~~transitions, with more solid water becoming liquid water ~~by~~through melting glacier/snow and more liquid water vaporized through ET (Z. Li et al., 2019; Yao et al., 2019). ~~Estimating~~Accurate estimation of ET at a large scale ~~around~~in the TP has always been challenging due to the ~~area's~~ high heterogeneity and the ~~harsh conditions~~complex topography. The TP is rich in land cover types, including grasslands, deserts, lakes, forests, glaciers, snow, and so on. The dynamics and thermodynamics of the sub-surface vary greatly among different climate types, making it a great challenge to conduct large-scale studies of ET processes on TP and explore the governing mechanism and feedback effect on the climate system and hydrological processes. In addition, the harsh natural conditions and ecological environment of the plateau make ground-based observations difficult, and the high cost of instrumentation and routine maintenance have resulted in a scarcity of ET ~~evapotranspiration~~ stations on the TP and a relatively short time series of observations (Ma et al., 2020).

~~ET estimation from land~~Land surface models (LSMs) and climate reanalysis ~~has~~have been widely ~~adopted, however~~used to estimate ET, but generally ~~with~~at coarse spatial resolutions (e.g., 0.25°) and ~~suffers~~suffer from large ~~accumulated~~cumulative errors due to many factors, e.g., the uncertainty of ~~driven forces~~forcing and model parametrization, surface heterogeneity, etc. (Chen et al., 2019; Khan et al., 2020; X. Li et al., 2019). In contrast, ET estimation based on satellite remote sensing observa-tions~~ that~~, which allow ~~for~~ high-resolutions estimation, has ~~obvious~~clear advantages, especially in the spatially heterogeneous regions of the TP (Ma et al~~.~~., 2006; Jia et al~~.~~., 2018; Zheng et al~~.~~., 2016). ~~During the last~~In recent decades, ~~the~~ remote sensing-

带格式的: 字体颜色: 自动设置

带格式的: 字体颜色: 自动设置
带格式的: 字体颜色: 自动设置
带格式的: 字体颜色: 自动设置
带格式的: 字体颜色: 自动设置
带格式的: 字体颜色: 自动设置
带格式的: 字体颜色: 自动设置
带格式的: 字体颜色: 自动设置
带格式的: 字体颜色: 自动设置
带格式的: 字体颜色: 自动设置
带格式的: 字体颜色: 自动设置
带格式的: 字体颜色: 自动设置
带格式的: 字体颜色: 自动设置
带格式的: 字体颜色: 自动设置
带格式的: 字体颜色: 自动设置

based ET datasets have been improved significantly, and several regional and global, high--quality ET datasets have been produced (e.g., Chen et al., 2021; Martens et al., 2017; Elnashar et al., 2021; Jia et al., 2018). For example, the validation results based on the global flux network show that the PMLV2 and ETMonitor global ET products have good accuracy (with RMSE<1mm/d) (Zhang et al., 2019b; Zheng and Jia, 2020). These improved ET datasets also have many advantages, e.g., the ability to distinguish different components (vegetation transpiration, soil evaporation, and canopy rainfall interception loss), higher spatial resolution (e.g., 1-km), better behaviorperformance in the heterogeneous land surface, but and their application to the Tibetan PlateauTP deserves further attention. However, previous studies also found significant differences between different products, such as divergentdifferent magnitudes of the annual mean ET in the TP ranging from 294 mm/yr (to 543 mm/yr (Chen et al., 2024; Wang et al., 2020) to 543 mm/yr (; Yuan et al., 2024; Zhang et al., 2018), and varyingdiverse trends of ET depending on the adopted datasets and study periods (Chen et al., 2024; Ma and Zhang, 2022; Wang et al.,., 2022). Inter-comparing different ET products certainly contribute to understand the ET process in TP, as well the ET magnitude and variations, which also there is a need to strengthen research on TP as a whole region and improve the understanding of the changing patterns of the Tibetan Plateau's water cycle and eco-hydrological processes (W. Wang et al., 2018).

The performance of ET product is related to both the adopted algorithms and the driving variables of the model (Mueller et al., 2013; Wang et al., 2022). Specifically, the contributions of different processes (e.g., plant transpiration, soil evaporation, water evaporation from canopy intercepted rainfall and open water bodybodies) to the total water flux of individual by different products also vary, most likely due to the theoretical and technological differences ofin different models and driving factors (Chen et al., 2021; Cui et al., 2020; Hu et al., 2009; Zhu et al.,., 2021, Ma and Zhang, 2022; Miralles et al., 2020). The global ET datasets based), Recent studies on satellite remote sensing were criticized for the lack of adaption to specificity for the special environment of TP and the uncertainty inherited from the input global meteorological reanalysis data, which may lead to a large uncertainty when directly applying the global ET in TP (Zou, 2020; Song et al. allake, 2017; Chang et al., 2018; Xue et al., 2013). These validations were generally based on either *in-situ* measurement by the eddy covariance system or the basin-scale ET estimated by water balance method, which represent the surface net water fluxevaporation suggest that integrates different processes (e.g., plant transpiration for the dense vegetation regions, snow sublimation for the dry snow cover periods for the eddy covariance system observations, even condensation when negative latent heat flux occurs), while these it accounts for about 4%-8% of the total annual ET from the whole TP (Wang et al., 2020; Chen et al., 2024). The comparison of different ET products mainly focus oncertainly contributes to the understand of the ET process in the TP, as well as the magnitude of ET and its spatiotemporal variability, including the ET components. There is also a need to enhance research on the whole TP as a region, and improve the understanding of the evolution of the ET (positive upward latent heat flux), which attributes towater cycle and eco-hydrological processes in the TP (W. Wang et al., 2018).validation uncertainty. In the evaluation of satellite remote sensing products against ground-based measurements and the inter-comparison between products, these specificities however are generally not included.

带格式的: 字体颜色: 自动设置
带格式的: 字体颜色: 自动设置
带格式的: 字体颜色: 自动设置
带格式的: 字体颜色: 自动设置
带格式的: 字体颜色: 自动设置
带格式的: 字体颜色: 自动设置
带格式的: 字体颜色: 自动设置
带格式的: 字体颜色: 自动设置
带格式的: 字体颜色: 自动设置
带格式的: 字体颜色: 自动设置
带格式的: 字体颜色: 自动设置
带格式的: 字体颜色: 自动设置
带格式的: 字体颜色: 自动设置

The performance of an ET product is related to both the adopted algorithms and the forcing variables (Mueller et al., 2013; Wang et al., 2022). The global ET datasets based on satellite remote sensing have been criticized for the lack of adaptation to the specificity of the TP environment and the uncertainty inherited from the input global meteorological reanalysis data, which may lead to a large uncertainty in the direct application of the global ET datasets for studies in the TP (Zou, 2020; Song et al., 2017; Chang et al., 2018; Xue et al., 2013). These evaluations have generally been based on either *in-situ* measurements using eddy covariance systems or the basin-scale ET estimates using water balance method, which represents the surface net liquid water flux at different scales, while ET products are estimates of the upward water vapour flux, which contributes to the uncertainty. Recently, Chen et al. (2024) evaluated several ET products with spatial resolutions ranging from 1km to 50km against site-scale eddy covariance observations. It is important to note that the observations from tower-based eddy covariance systems have a very small footprint (approximately several hundred metres depending on weather conditions), and direct comparison of site-scale observations with the coarse-resolution ET products (e.g., 25km) is problematic due to the severe problem of spatial mismatch. In order to increase the credibility of currently available ET products, this study will undertake a more comprehensive evaluation, taking into account both *in-situ* observations and basin-scale measurements.

带格式的: 字体颜色: 自动设置

带格式的: 字体颜色: 自动设置

The following questions should be addressedemerge from this brief literature review: 1) How accurate are these improved ET products, and how well do different products agree to capture the ET magnitude and variability of ET in the TP? 2) How much water is vaporized in the TP and which processes, e.g., plant transpiration, soil evaporation, snow/ice sublimation, play a significant role? 3) How do different products respond to environmental factors, e.g., precipitation? Answering these questions would reveal the strengths and weaknesses of different ET products and address the knowledge gaps on relevant processes overin the TP, which isare fundamental for differentvarious scientific and practical purposes.

The aim of this paper is to clarify the ET magnitude and variability of ET in the TP by assessing and inter-comparing the accuracy and spatiotemporal variationsvariability of ET overin the TP from commonaccording to commonly available gridded products. Specifically, the main objectives includeare 1) to estimate the absolute uncertainties of individual ET products using flux tower data and water balance estimates; 2) to evaluate and compare the spatiotemporal variationsvariability of total ET and its components of ET between from different ET products; 3) to assess the response of ET in TP to the environmental factors. To estimate the absolute uncertainty of the different ET data products, we will use a validation approach using data from flux towers and water balance estimates. Afterwards, to evaluate the spatiotemporal variations and partitioning, we will intercompare the spatial variation of the different ET products using both multiple-year averaged annual ET and the seasonal variation of ET. Finally, we will assess the response of ET in TP to precipitation, net surface radiation and leaf area index based on the Pearson correlation analysis. .

2 Methodology and Data

2.1 Study region

The Tibetan Plateau (25-40°N, 70-105°E) is the highest elevated region in the world, covering an area of approximately 3.0 million km^2, with most ~~region~~areas above 2,500 meters ~~in altitude~~ (Figure 1). It has complex climatic regimes, ~~including~~ranging from a humid~~, semi-humid, monsoon, semi-arid, arid, and~~ climate with an aridity ratio less than 0.3 to hyper-arid ~~climates.~~climate with an aridity ratio larger than 3 (Feng et al., 2024). The climate is influenced by both westerly and the Asian monsoon, which is also enhanced by the thermal forcing of the TP (Zhou et al., 2009; Wu et al., 2012; Yang et al., 2014). Influenced by multiple sources of water vapor ~~sources~~ through atmospheric circulation and alpine terrain, its precipitation ~~presents~~shows spatial variability with the average annual precipitation gradually increasing from less than 50 mm/yr in the northwest to more than 1000 mm/yr in the southeast, and most of the precipitation is concentrated in summer (Jiang et al., 2023). The TP is also known for its extensive snow and glacier ~~coverage~~cover, with a total glacier area of approximately 50,000 km^2 (Yao et al., 2007) and 77% of the area above ~~6000m above sea level~~6000 m is covered by snow (Chu et al~~.~~., 2023). The main land cover types are ~~mainly~~ forest, grassland, bare soil, glaciers and snow (Supplementary Figure S1). The water supply for the dense river network on the TP, which includes the headwaters of five major Asian rivers, is ~~primarily formed by~~mainly precipitation and ~~the~~ meltwater from glaciers and snowpack.

The TP region ~~comprises~~consists of 12 subregions: Hexi, Tarim, Qaidam, Upper Amu Darya, Inner TP, Upper Yellow, Upper Yangtze, Upper Salween, Upper Mekong, Upper Brahmaputra, Upper Ganges, and Upper Indus (Figure 1). The first five subregions, Hexi, Tarim, Qaidam, Amu Darya, and Inner TP, are located in the northern, western, and central parts of the TP and ~~experience~~receive relatively low precipitation. The remaining watersheds receive high precipitation due to the monsoons originating from the Arabian Sea, the South China Sea, and the Western Pacific, and ~~extreme~~extremely high annual precipitation (>~~1000mm~~1000 mm/yr) ~~are~~is found in the Upper Salween, Upper Brahmaputra, and Upper Ganges river basins.

带格式的: 字体颜色: 自动设置
带格式的: 字体颜色: 自动设置
带格式的: 字体颜色: 自动设置
带格式的: 字体颜色: 自动设置
带格式的: 字体颜色: 自动设置
带格式的: 字体颜色: 自动设置
带格式的: 字体颜色: 自动设置
带格式的: 字体颜色: 自动设置
带格式的: 字体颜色: 自动设置
带格式的: 字体颜色: 自动设置
带格式的: 字体颜色: 自动设置
带格式的: 字体颜色: 自动设置
带格式的: 字体颜色: 自动设置
带格式的: 字体颜色: 自动设置
带格式的: 字体颜色: 自动设置
带格式的: 字体颜色: 自动设置
带格式的: 字体颜色: 自动设置
带格式的: 字体颜色: 自动设置
带格式的: 字体颜色: 自动设置
带格式的: 字体颜色: 自动设置
带格式的: 字体颜色: 自动设置
带格式的: 字体颜色: 自动设置
带格式的: 字体颜色: 自动设置
带格式的: 字体颜色: 自动设置
带格式的: 字体颜色: 自动设置
带格式的: 字体颜色: 自动设置
带格式的: 字体颜色: 自动设置

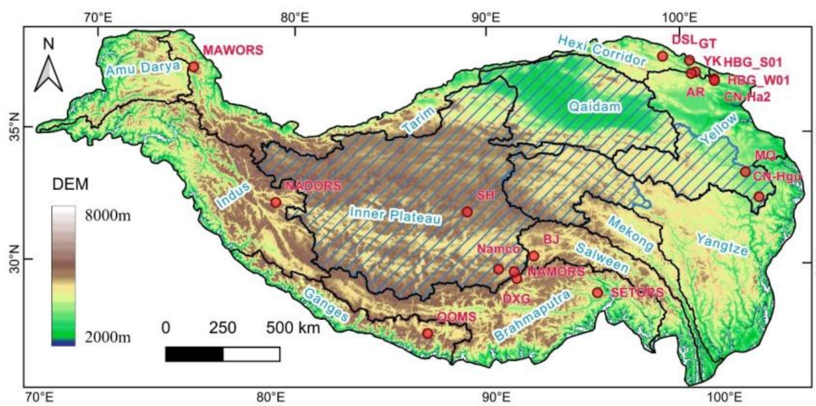

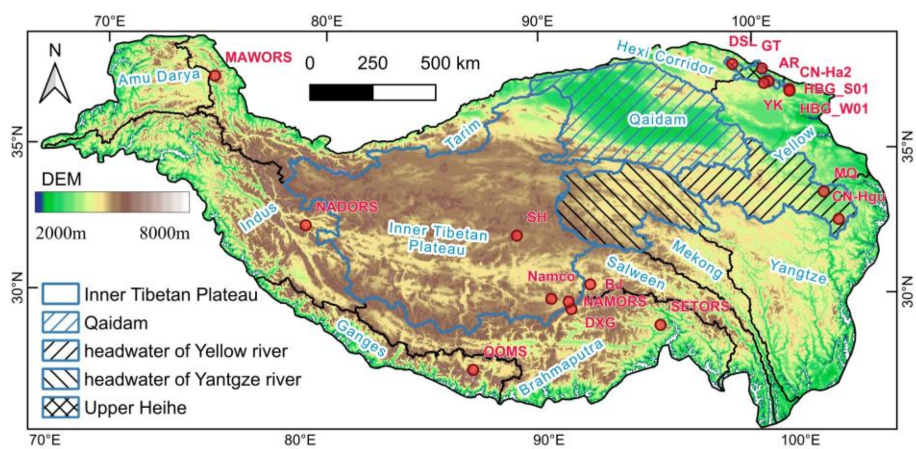

Figure 1: Location of the selected ground flux tower observation sites and major river basins in the ~~Tibetan Plateau~~TP, with elevation shown as background. The selected basins where the evaluation of ET products using water balance-based data was carried out are also shown.

2.2 Data sources

2.2.1 Flux tower data

To validate ET at high spatial resolution (≤ 1km), measurements of near-surface turbulent fluxes by the eddy-covariance method at 18 flux towers were collected. The measurements were aggregated to total monthly ET to carry out the evaluation study. Figure 1 presents the spatial distribution of these sites, and the details are provided in Table 1. The quality of flux observation data at each site was evaluated after data screening, and only reliable observations were selected following the methodology described by Zheng et al. (2022). ~~These the~~The sites, where gap-filled daily or monthly ET data with reliable quality were already available ~~(~~, i.e., DXG, HBG-S01, HBG-W01, CN-HaM, CN-Hgu, SH~~,~~ and Maqu~~),~~, were directly adopted without further ~~modification~~modifications. For sites that provide half-hourly or hourly data, the observed latent heat flux data were gap-filled after energy closure correction, and this includes six sites (BJ, NADORS, SETORS, QOMS, NAMORS, MAWORS) from the Tibetan Observation and Research Platform (Ma et al., 2020; 2008), four sites from the Heihe Integrated Observatory Network (Liu et al., 2018; Li et al., 2009), and our own site at Namco. The Bowen ratio energy balance correction method preserves the Bowen ratio by attributing the residual term of the energy balance to the latent heat flux and sensible heat flux (Twine et al., 2000; Foken, 2008; Chen et al., 2014). The corrected half-hourly or hourly LE data was then averaged to ~~obtaine~~obtain daily ET values, and only the days with more than 80% of the hourly flux were retained as valid observations. The missing daily ET values were further filled using the constant reference evapotranspiration fraction method (Jiang et al., 2022). The monthly ET was finally calculated by accumulating the daily ET values, and those months with less than 50% valid daily ET values were ~~excluded~~treated as missing values. The missing data was not further filled, and it was not used for validation to avoid the impact of uncertainty introduced by gap-filling.

Table 1: List of ground flux tower observation sites.

Site Code	Site Name	Latitude/Longitude	Elevation	Land Cover	Periods	Sources / reference
MAWORS	TORP MAWORS	38.41 ºN, 75.05 ºE	3668	Desert steppe	2012-2016	Ma et al., 2020
NADORS	TORP NADORS	33.39 ºN, 79.70 ºE	4270	Desert steppe	2010–2018	Ma et al., 2020
NAMORS	TORP NAMORS	30.77 ºN, 90.96 ºE	4730	Alpine steppe	2008–2018	Ma et al., 2020
QOMS	TORP QOMS	28.36 ºN, 86.95 ºE	4298	Desert steppe	2007–2018	Ma et al., 2020
SETORS	TORP SETORS	29.77 ºN, 94.74 ºE	3327	Alpine meadow	2007–2018	Ma et al., 2020
BJ	TORP BJ	31.37 ºN, 91.90 ºE	4509	Sparse alpine meadow	2010–2016	Ma et al., 2020
SH	TORP Shuanghu	33.21 ºN, 88.83 ºE	4947	Alpine steppe	2013–2018	Ma et al., 2015
ARS	HiWATER A'rou	38.05 ºN, 100.46 ºE	3033	Dense alpine meadow	2008–2018	Liu et al., 2018
DSL	HiWATER Dashalong	38.84 ºN, 98.94 ºE	3739	Alpine meadow	2013-2018	Liu et al., 2018
YK	HiWATER Yakou	38.01 ºN, 100.24 ºE	4148	Alpine steppe	2014-2018	Liu et al., 2018

GT	HiWATER Guantan	38.53 ºN, 100.25 ºE	2835	Needleleaf forest	2009-2011	Li et al., 2009
DXG	ChinaFLUX Dangxiong	30.49 ºN, 91.07 ºE	4333	Alpine meadow	2004–2010	Yu et al., 2006
HBG-S01	ChinaFLUX Haibei grassland	37.67 ºN, 101.33 ºE	3358	Dense alpine meadow	2003-2010	Yu et al., 2006
HBG-W01	ChinaFLUX Haibei wetland	37.61 ºN, 101.33 ºE	3357	Alpine wetland	2004-2009	Zhang et al., 2020
CN-Ha2	FLUXNET Tibet Haibei Alpine	37.37 ºN, 101.18 ºE	3824	Alpine meadow	2002-2004	Kato et al., 2004
CN-Hgu	FLUXNET-CH4 CN-Hgu Hongyuan	32.85 ºN, 102.59 ºE	3500	Alpine meadow	2015-2017	Niu and Chen, 2020
MQ	Maqu site	33.89 ºN, 102.14 ºE	3423	Dense alpine meadow	2013-2016	Shang et al., 2015
Namco	Namco site	30.89 ºN, 90.24 ºE	4760	Alpine steppe	2019-2021	this study

带格式的: 字体颜色: 自动设置
带格式的: 字体颜色: 自动设置
带格式的: 字体颜色: 自动设置
带格式的: 字体颜色: 自动设置
带格式的: 字体颜色: 自动设置
带格式的: 字体颜色: 自动设置
带格式的: 字体颜色: 自动设置
带格式的: 字体颜色: 自动设置

2.2.2 Water balance-based ET data

We also collected monthly water balance-based evapotranspiration (ET_{wb}) from other studies at the basin-scale to evaluate the accuracy of ET data products at monthly scale. Compared to the flux tower data, ET_{wb} can also be used to evaluate the products with coarse spatial resolution (≥5km). The monthly ET_{wb} may also contain uncertainties due to propagated errors from precipitation and water storage, although ET_{wb} is often considered as the 'ground truth' for validating basin-wide ET estimates. In total, monthly ET_{wb} from five river basins were extracted from previous studies (Ma and Zhang., 2022; Wang et al., 2021), including the headwaters of the Yellow basin (HYE), the headwaters of Yangtze basin (HYA), the Inner TP (INTP), Qaidam (QDM) basins, and the upper Heihe basin (UH), as shown in Figure 1 and Table 2.

Table 2: Basins with water balance-based ET data for validation.

Basin name	Periods	Area (km^2)	Runoff gauging station	Description of the dataset used for water balance-based ET estimation	Sources /reference
Headwaters of Yellow basin (HYE)	2003-2015	122,890	Tangnaihai	Precipitation was from the ensemble mean of CMFD (https://doi.org/10.11888/AtmosphericPhysics.tpe.249369.file), CN05.1 (http://data.cma.cn), and MSWEP (http://www.gloh2o.org/mswep/). Terrestrial water storage changes were derived from the Gravity Recovery and Climate Experiment (GRACE) (https://grace.jpl.nasa.govs/). Monthly ET_{wb} was turned into zero whenever it is negative, and ET from lakes was excluded.	Ma and Zhang., 2022
Headwaters of Yangtze basin (HYA)	2003-2015	140,270	Zhimenda		
Inner Tibet Plateau (INTP)	2003-2015	708,252	- (endorheic river)		
Qaidam (QDM)	2003-2015	253,252	- (endorheic river)		
Upper Heihe basin (UH)	2004-2008	10,011	Yingluoxia	Precipitation was from MSWEP after comparing with five datasets. Terrestrial water storage changes were derived from GRACE.	Wang et al. 2022

2.2.3 ET products

This study examined 22 ET datasets (including 20 global datasets and 2 regional datasets) (Table ~~2~~3), and detailed descriptions of ~~each~~ ET data can be found in ~~SI~~Appendix I in Supplementary materials. Among these~~ datasets~~, 7 datasets were ~~with~~at high spatial resolution (≤1km), including ETMonitor (Zheng et al., 2022), MOD16 (Mu et al., 2011), MOD16-STM (Yuan et al., 2021), the Penman–Monteith–Leuning Version 2 (PMLV2) (Zhang et al., 2019), the operational Simplified Surface Energy Balance (SSEBop) (Senay et al., 2020), GLASS (Yao et al., 2014), and SynthesisET (Elnashar et al., 2021). Most of these high-resolution ET datasets used~~ the~~ different variables or indices from Moderate Resolution Imaging Spectroradiometer (MODIS) as main inputs. Two products (GLASS, SynthesisET) are ensemble ET products generated by fusing other ET models or datasets. Remote sensing ET datasets with coarse resolution were also collected, including Thermal Energy Balance (EB) ET (Chen et al., 2021), Breathing Earth System Simulator version 2 (BESSv2) (Li et al., 2023), GLEAM (version 3.5a based on satellite and reanalysis data with long-term coverage, and version 3.5b based on mainly satellite data) (Martens et al., 2017), and FLUXCOM (RS version using MODIS remote sensing data as input, and RS_METEO version using remote sensing and meteorological data as input) (Jung et al., 2019). MOD16-STM and PMLV2-Tibet are regional ET datasets that were calibrated against ground-based eddy-covariance measurements on the TP. MOD16-STM is an enhanced version of the MOD16 algorithm by redefining the transpiration and soil evaporation module (Yuan et al., 2021), while PMLV2-Tibet is a calibrated version of PMLV2 (Ma and Zhang, 2022). We also collected some ET products based on land surface models and climate reanalysis datasets, including calibration-free complementary relationship (CR) ET (Ma et al., 2021), TerraClimate (Abatzoglou et al., 2018), MERRA2 (Gelaro et al., 2017), ERA5 (Hersbach et al., 2020), ERA5-Land (Muñoz-Sabater et al., 2021), GLDAS-VIC (Rodell et al., 2004), GLDAS-Noah (Rodell et al., 2004), GLDAS-~~S~~CLSM (B. Li et al., 2019). In summary, among these evaluated ET products, there are 14 products that primarily use remote sensing products, including 2 products (SSEBop and EB) based on land surface temperature (LST), 8 products (ETMonitor, MOD16, MOD16-STM, PMLV2, PMLV2-Tibet, GLEAMv35a, GLEAMv35b, BESSv2) based on PM-types models (including Penman-Monteith equation, Priestley-Taylor equation, Shuttleworth-Wallace equation), 4 products (FLUXCOM-RS, FLUXCOM-RS-METEO, GLASS, SynthesisET) based on data-driven methods. Among the 8 PM-type models, there are 3 models that incorporate soil moisture to account for the influence of available soil water on ET, including ETMonitor, GLEAMv35a, and GLEAMv35b.

All products were temporally aggregated to monthly total ET from their native temporal resolutions prior to evaluation. For the daily resolution products, simple summation operations were performed to obtain the monthly ET values. For 8-day resolution data, a mean daily ET value was first estimated with the available data in that month, and the monthly ET value was then obtained by multiplying the mean daily values by the number of days in the month.

Table ~~2~~3: List of ~~ground flux tower observation sites~~ET products evaluated in this study.

带格式的: 字体颜色: 自动设置
带格式的: 字体颜色: 自动设置
带格式的: 字体颜色: 自动设置
带格式的: 字体颜色: 自动设置
带格式的: 字体颜色: 自动设置
带格式的: 字体颜色: 自动设置
带格式的: 字体颜色: 自动设置
带格式的: 字体颜色: 自动设置
带格式的: 字体颜色: 自动设置
带格式的: 字体颜色: 自动设置
带格式的: 字体颜色: 自动设置
带格式的: 字体颜色: 自动设置
带格式的: 字体颜色: 自动设置
带格式的: 字体颜色: 自动设置
带格式的: 字体颜色: 自动设置
带格式的: 字体颜色: 自动设置
带格式的: 字体颜色: 自动设置
带格式的: 字体颜色: 自动设置
带格式的: 字体颜色: 自动设置
带格式的: 字体颜色: 自动设置
带格式的: 字体颜色: 自动设置
带格式的: 字体颜色: 自动设置
带格式的: 字体颜色: 自动设置

Products	**Temporal resolution**	**Spatial resolution**	**Temporal coverage**	**Basic principle ~~and approach~~or algorithm**	**Main forcing data**	**ET components**	**Validation method**	**Reference**
ETMonitor	Daily	1km	2000-2021	~~ETMonitor model with multi-parameterizations for different processes including plant transpiration, soil evaporation, evaporation from canopy intercepted rainfall and open water body, sublimation from snow/ice~~ Shuttleworth–Wallace model combined with Jarvis-type method for Ec and Es, revised Gash model for Ei, Penman-Monteith equation for Ew and Ess.	ERA5 meteorological data, GLASS (LAI, FVC, albedo), MODIS land cover, dynamic water and snow cover, downscaled ESA-CCI soil moisture.	Ec, Es, Ei, Ew, Ess	~~Both~~ ground observation and ~~water balance estimation~~ ET_{wb}	Zheng et al., 2022
MOD16	8-day	500m	2000- present	MOD-PM based algorithm for vegetation covered region.	NASA GMAO meteorological data, MODIS (land cover, LAI).	Ec, Es, Ei	~~Both~~ ground observation and ~~water balance estimation~~ ET_{wb}	Mu et al., 2011
PMLV2	8-day	500m	2002-2019	Penman-Monteith-Leuning model V2 using remote-sensing as input.	GLDAS meteorological data, MODIS (land cover, LAI, albedo, emissivity).	Ec, Es, Ei, Ew	~~Both~~ ground observation and ~~water balance estimation~~ ET_{wb}	Zhang et al., 2019
SSEBop	10-day	1km	2002-2019	Operational Simplified Surface Energy Balance using satellite psychrometric principle.	Daymet Ta, and GLDAS PET data, MODIS (NDVI, LST, albedo).	-	~~Both~~ ground observation and ~~water balance estimation~~ ET_{wb}	Senay et al., 2020
GLASS	8-day	1km	2000-2018	Bayesian multi-model ensemble of different ET products.	MOD16 ET, PT-JPL ET, and other ET datasets	-	~~Both~~ ground observation and ~~water~~	Yao et al., 2014

							~~balance estimation~~ET_{wb}	
SynthesisET	Monthly	1km	1982-2019	Synthetization of different ET products based on ranking of validation metrics.	MOD16 ET, PML ET, SSEBop ET, GLEAM ET, GLDAS ET, etc.	-	~~Both~~ ground observation and ~~water balance estimation~~ET_{wb}	Elnashar et al.~~,~~, 2021
MOD16-STM	Monthly	1km	~~2000~~1982-2018	Enhanced MOD16 algorithm by redefining the transpiration and soil evaporation module. MODIS yearly constant land cover is used to extract water cover.	Regional CMFD meteorological data, ERA5-Land LST, GLASS albedo and emissivity, AVHRR NDVI, GLEAM soil moisture.	Ec, Es, Ei	~~Both~~ ground observation and ~~water balance estimation~~ET_{wb}	Yuan et al.~~,~~, 2024; Yuan et al., 2021
PMLV2-Tibet	8-day	5km	1982-2016	Penman-Monteith-Leuning V2 model calibrated in the Tibet Plateau	~~water balance estimation~~ Regional CMFD meteorological data, ERA5-Land LST, GLASS albedo, GLASS and GIMSS LAI.	-	ET_{wb}	Ma et al.~~,~~, 2022
EB	Daily~~Monthly~~	0.05°	2000-2017	Improved Surface Energy Balance method based monthly LST	~~water balance estimation~~ ERA-Interim meteorological data, GLASS (LAI, FVC, albedo), MODIS (land cover, LST).	-	ET_{wb}	Chen et al.~~,~~, 2021
BESSv2	Monthly~~monthly~~	5km	1982-2019	Quadratic form of the Penman-Monteith equation to estimate ET uses various satellite remote-sensing as input	~~water balance estimation~~ ERA5 meteorological data, GLASS (LAI, albedo), MODIS (land cover, cloud, aerosol, LAI, etc.).	Ec, Es, Ei	ET_{wb}	Li et al.~~,~~, 2023
FLUXCOM-RS	8-day	0.0833°	2001-2015	FLUXNET and ensemble multiple machine learning	~~water balance estimation~~Multiple meteorological data, MODIS (land cover, LST, fPAR, NDVI, EVI, NDWI).	-	ET_{wb}	Jung et al.~~,~~, 2019
FLUXCOM-RS-METEO	8-day	0.5°	2001-2013	FLUXNET and ensemble multiple machine learning	~~water balance estimation~~Multiple meteorological data.	-	ET_{wb}	Jung et al.~~,~~, 2019
GLEAMv3.5a	Daily	0.25°	1980-2018	Priestley-Taylor equation and data assimilation of soil moisture	~~water balance estimation~~ ERA5 meteorological data, ESA-CCI soil moisture,	Ec, Es, Ei, Ew, Ess	ET_{wb}	Martens et al.~~,~~, 2017

带格式的: 字体颜色: 自动设置
带格式的: 字体颜色: 自动设置
带格式的: 字体颜色: 自动设置, 法语(法国)
带格式的: 字体颜色: 自动设置, 法语(法国)
带格式的: 法语(法国)
插入的单元格
带格式的: 字体颜色: 自动设置
带格式的: 字体颜色: 自动设置
带格式的: 字体: 倾斜
带格式的: 字体颜色: 自动设置
带格式的: 字体颜色: 自动设置
带格式的: 字体: 倾斜
带格式的: 字体颜色: 自动设置
带格式的: 字体颜色: 自动设置
带格式的: 字体: 倾斜, 意大利语(意大利)
带格式的: 字体颜色: 自动设置
带格式的: 字体颜色: 自动设置
带格式的: 字体: 倾斜
带格式的: 字体颜色: 自动设置
带格式的: 字体: 倾斜
带格式的: 字体颜色: 自动设置
带格式的: 字体颜色: 自动设置
带格式的: 字体颜色: 自动设置

					NSWEP precipitation, GLOBSNOW SWE， etc.			
GLEA Mv3.5b	Daily	0.25°	2003-2018	Priestley-Taylor equation and data assimilation of soil moisture	water balance estimation CERES radiation, AIRS temperature, NSWEP precipitation, GLOBSNOW SWE.	Ec, Ei, Ew, Ess	ET_{wb}	Martens et al., 2017
CR	Monthly	0.25°	1982-20182000-2022	calibration-free complementary relationship model	water balance estimation ERA5 meteorological data, ERA5-Land LST, GLASS albedo, CERES net radiation.	-	ET_{wb}	Ma et al., 2021
GLDAS-CLS-MTerra Climate	Dai-lyMonthly	0.25°	2003-present1958-2020	modified Thornthwaite-Mather climatic water balance modelGlobal Land Data Assimilation System, Catchment Land Surface Model (GLDAS_CLSM025_DA1_D.2.2)	water balance estimationGLDAS-v2.2 forcing data from ECWMF and Princeton, GRACE TWS data.	Ec, Es, Ei, Ess	ET_{wb}	B. LiAbatzoglou et al., 20182019
GLDAS-CLS-MNoah	Month-lyDaily	0.25°	20032000-present	Global Land Data Assimilation System, Catchment Version 2, Noah Land Surface Model (GLDAS_CLSM025_DA1_D.2NOAH025_3H.2.1)	water balance estimationGLDAS-v2.1 forcing data, combination of GDAS, disaggregated daily GPCP precipitation, and AFWA radiation datasets.	Ec, Es, Ei	ET_{wb}	RodellB. Li et al., 20192004
GLDAS-Noah-VIC	Monthly	1°0.25°	2000-present	Global Land Data Assimilation System Version 2.1, Noah Land Surface Model (GLDAS_NOAH025_3HVIC10_3M.2.1)	water balance estimationGLDAS-v2.1 forcing data, combination of GDAS, disaggregated daily GPCP precipitation, and AFWA radiation datasets.	Ec, Es, Ei	ET_{wb}	Rodell et al., 2004
Terra-Cli-mateGLDAS-VIC	Monthly	0.25°1°	1958-20202000-present Global Land Data Assimilation System Version 2.1, Noah Land Surface Model (GLDAS_VIC10_3M.2.1)	modified Thornthwaite-Mather climatic water-balance estimationmodel	Meteorological data from WorldClim, CRU, JRA, etc.	-	ET_{wb}	RodellAbatzoglou et al., 20042018

带格式的: 字体: 倾斜, 意大利语(意大利)
带格式的: 字体颜色: 自动设置
带格式的: 字体颜色: 自动设置
带格式的: 字体: 倾斜
带格式的: 字体颜色: 自动设置
带格式的: 字体颜色: 自动设置
带格式的: 字体: 倾斜, 意大利语(意大利)
带格式的: 字体颜色: 自动设置
带格式表格
带格式的: 字体颜色: 自动设置
带格式的: 字体: 倾斜
带格式的: 字体颜色: 自动设置
带格式的: 字体颜色: 自动设置
带格式的: 字体颜色: 自动设置
带格式的: 字体: 倾斜
带格式的: 字体颜色: 自动设置
带格式的: 字体: 倾斜
插入的单元格
带格式的: 两端对齐
带格式的: 字体颜色: 自动设置
带格式的: 字体颜色: 自动设置

MERRA2	Monthly	0.25º	1979-present	theThe Modern-Era Retrospective analysis for Research and Applications, Version 2, by NASA Global Modeling and Assimilation Office (GMAO) using the Goddard Earth Observing System Model (GEOS)	water balance estimation MERRA-2 global atmospheric reanalysis data	Ec, Es, Ei, Ew, Ess	ET_{wb}	Gelaro et al., 2017
ERA5	Monthly	0.25º	1979- present	The fifth generation of European ReAnalysis of ECMWF based on Hydrology Tiled ECMWF Scheme for Surface Exchanges over Land (HTESSEL).	water balance estimationECMWF ERA5 global climate reanalysis data.	-	ET_{wb}	Hersbach et al., 2020
ERA5-Land	Monthly	0.25º	1979- present	newNew land component of the fifth generation of European ReAnalysis of ECMWF: Carbon Hydrology-Tiled ECMWF Scheme for Surface Exchanges over Land (CHTESSEL).	water balance estimationDownscaled meteorological forcing from the ERA5 climate reanalysis	-	ET_{wb}	Muñoz-Sabater et al., 2021

带格式的: 字体颜色: 自动设置

带格式表格

带格式的: 字体颜色: 自动设置

带格式的: 字体颜色: 自动设置

2.2.3 Water balance-based ET data

We also collected water balance-based evapotranspiration (ET_{wb}) from other studies at the basin-scale to evaluate the accuracy of ET data products. Compared with the flux tower data, ET_{wb} can also be used to validate these products with coarse spatial resolution (≥5km). The monthly ET_{wb} may also involve uncertainties because of the propagated errors from precipitation and water storage, although ET_{wb} is often considered as 'ground truth' for validating basin-wide ET estimates. Totally, monthly ET_{wb} from five river basins were extracted from previous studies (Ma and Zhang., 2022; Wang et al. 2021), including the headwaters of Yellow basin, headwaters of Yangtze basin, upper Heihe basin, and two endorheic basins (Inner Tibet Plateau, Qaidam basins), as shown in Figure 1.

2.2.4 Other data

The precipitation data adoptedused in this study isare from the TPHiPr dataset, which is a long-term high-resolution (1/3°, daily) precipitation datasets for the TP obtained by merging the atmospheric model output with gauge observations from more than 9000 rain gauges around the TP (Jiang et al.,, 2023). Compared to other widely used precipitation datasets, this dataset has remarkably better accuracy in the TP, with a generally unbiased and root mean square error of 5.0 mm/d. The leaf area index (LAI) data is from the Global Land Surface Satellite (GLASS) data products (Xiao et al., 2014, 2022). GLASS LAI has a spatial resolution of 500m, which were spatially aggregated to 1-km resolution in this study.

带格式的: 字体颜色: 自动设置

带格式的: 字体颜色: 自动设置

~~The effect of net radiation (Rn) on ET is explored. The grid Rn data used in this study were obtained from Zheng et al. (2022), which calculated Rn as the difference between incoming and outgoing radiation fluxes both in shortwave and longwave based on mainly GLASS albedo and ERA5 data. The adopted Rn has an RMSE value of 30.75 W/m^2 when validated against ground measurements (Zheng et al. 2022), which is comparable to the RMSE of 33.56 W/m^2 for CERES (Clouds and the Earth's Radiant Energy System) Rn products (Jia et al., 2016).~~

2.3 Methodology

2.3.1 Evaluation of ET products ~~validation~~

We ~~fist validate the ET from~~evaluated different ET data products (~~refer to~~ Table 2) at monthly scale against ground observations and basin-scale estimates of the water balance~~, and various accuracy indicators~~. Various error metrics were calculated to assess the ~~performance~~accuracy of these ET datasets. These ET datasets were ~~selected as the~~ mainstream gridded ET products obtained by a variety of ~~typical~~ algorithms applied ~~in~~to the TP or globally. Considering that the footprint of the *in-situ* flux tower observations was generally ~~within~~in the range of several hundred meters to kilometers, they were ~~adopted~~used to ~~validate~~evaluate ET datasets at relatively high resolution (≤1km~~)~~), including six global ET products and one regional ET ~~products, including~~product, i.e., ETMonitor, MOD16, PMLV2, SSEBop, GLASS, SynthesisET, and MOD16-STM~~, while all~~. All products were ~~validated based on~~evaluated against estimates of the basin-scale water balance ~~estimation.~~, regardless of their spatial resolution. When validating with ground observations, the ET values ~~from~~of the ET products in the pixels where the flux sites are located were ~~directly~~ extracted directly for comparison. ~~When comparing~~For comparison with ~~ET_{wb} data,~~the basin-scale water balance data, the basin-scale monthly averaged ET ~~by~~values of different products were calculated using the area-~~weight average~~weighted averaging method according to the basin boundary.

带格式的: 字体颜色: 自动设置

The following commonly used accuracy ~~indicators are employed~~metrics were applied, including the correlation coefficient (R), the bias (BIAS), the root mean square error (RMSE), and the Kling-Gupta efficiency (KGE) (Gupta et al., 2009). The KGE is a multi-objective statistical indicator ~~incorporating~~that incorporates the correlation, relative variability ratio and mean ~~values~~value ratio, to ~~assess the performance~~ comprehensively~~. KGE was~~ evaluate the accuracy. The metrics were calculated as:

带格式的: 字体颜色: 自动设置

~~$$KGE = 1 - \sqrt{(R-1)^2 + (\frac{\mu(ET_e)}{\mu(ET_o)} - 1)^2 + (\frac{\sigma(ET_e)}{\sigma(ET_o)} - 1)^2}, \quad (1)$$~~

$$R = \frac{\sum_{i=1}^{n}(ET_e - \overline{ET_e})(ET_o - \overline{ET_o})}{\sqrt{\sum_{i=1}^{n}(ET_e - \overline{ET_e})^2}\sqrt{\sum_{i=1}^{n}(ET_o - \overline{ET_o})^2}} \quad (1)$$

$$BIAS = \sum_{i=1}^{n}(ET_e - ET_o)/n \quad (2)$$

$$RMSE = \sqrt{\sum_{i=1}^{n}(ET_e - ET_o)^2} \quad (3)$$

$$KGE = 1 - \sqrt{(R-1)^2 + (\frac{\mu(ET_e)}{\mu(ET_o)} - 1)^2 + (\frac{\sigma(ET_e)}{\sigma(ET_o)} - 1)^2} \quad (4)$$

where ET_e (mm/month) indicates the ET values of different products, ET_o (mm/month) indicates the ground-truth ET values, either from *in-situ* observations or basin-scale water balance ~~estimation~~estimates, μ is the mean value, σ is the standard deviation, and R is the Pearson correlation coefficient between the ET values and the ground-truth ET values. KGE is smaller than 1, and higher KGE means better agreement between ~~the observed and the simulated results generally~~observations and estimates.

2.3.2 Inter-comparison of different products

~~To~~In order to inter-compare the spatial variation of ET by different products, multiple-year ~~averaged~~average annual ET was ~~estimated~~calculated and analysed for each product during their overlap period ~~(~~from 2003 ~~~ 2015).~~to 2013, unless specific period was redefined. The averaged and median values of ET, as well as the ~~stand~~standard deviation, ~~by~~of different products were ~~estimated~~calculated at both pixel-wise and basin-wise level, to ~~express~~explore the discrepancy of ET magnitude by different products. The ratio of standard deviation to multi-products ~~averaged~~average ET values was ~~estimated to present the~~used as an indicator of uncertainty. For products that also provide the ET components~~, including~~ (i.e., plant transpiration, soil evaporation, canopy rainfall interception evaporation, open water evaporation, and snow/ice sublimation~~,~~), the ~~separate contribution~~individual contributions of these components to the total ET ~~are~~were also calculated and compared.

~~To compare the seasonal variation of~~Monthly ET~~, monthly climatology was~~ values were produced ~~by calculating the mean value for each month~~ for each product~~.~~ to analyse the seasonal variation in ET. It is generally agreed that long-term temporal coverage (i.e., at least 30 years) is required ~~when analyzing~~to estimate the trend of climate variables. However, most ET products cover a relatively short period~~ in this study.~~. Although the ~~relative~~relatively short period of time ~~may~~can be debated, these time series are helpful to clarify the trend ~~of annual ET by each product was detected using robust regression to compare the annual variation of ET by differen~~tin recent years and to understand the difference in trend among products.

~~**2.3.3 Response of ET to different environmental factors**~~

~~To investigate~~The calculation of the trends can be affected by exceptional years (outliers) with extremely high or low ET. To reduce the ~~impact of environmental factors on~~influence of these outliers, we used the ~~variation of ET,~~ robust regression method instead of the ~~Pearson correlation analysis was conducted to measure how annual ET responds to its main governing environmental factors, including precipitation, LAI, and net radiation. These variables were selected to represent~~ simple linear regression method. The significance level of the ~~strength of the water cycle, energy budget, and plant physiology, which are the three main processes regulating ET.~~trend was estimated using a *t*-test.

带格式的: 字体: 倾斜

带格式的: 字体: 非倾斜

带格式的: 段落间距段后: 0 磅

3. Results

3.1 Evaluation of ET products

3.1.1 Validation of ET products against flux tower measurements

Figure 2 and Supplementary Figure S2 ~~present~~show the validation results. It should be ~~noticed~~noted that all the products have different temporal ~~and spatial~~ coverage and the eddy covariance observations at the flux tower sites also cover different years. In addition, some ET products do not have valid values over certain land cover types, e.g~~.,~~., the MOD16 ET ~~product~~algorithm does not ~~provide data in~~ work over non-~~vegetation covered pixels (hence no~~ vegetated areas, so MOD16 ET has no data ~~for sites of~~at the QOMS and NADORS~~),~~ sites (both have land cover as desert steppe). Therefore, the accuracy metrics for each ET product in Figure 2 have only be calculated for those periods when both ground measurements and the ~~validation results are obtained primarily based on~~ ET product data are available at each site. To provide a ~~different number of samples for different products. To have a fairer~~fair and overall comparison, Figure 2 also shows the ~~indicators when using same validation samples for all the products, which was conducted by limiting the validation samples only at the vegetation covered sites during 2001~2018.~~ metrics for the condition only when all products and ground data are overlapped (‘*Overlap*’) and the overall metrics that include all conditions (‘*All*’). More information on the validation period and relevant information can be found in Supplementary Table S1.

~~As anticipated, the regional ET product (MOD16-STM) demonstrated good accuracy with low RMSE and high KGE (15.84mm/month and 0.77 when using the same validation samples). This may be attributed to the fact that MOD16-STM ET was calibrated using the flux observation and was retrieved based on the regional bias-corrected climate data with better accuracy than the global forcing data.~~ Among all the global ET datasets, ETMonitor and PMLV2 ET achieved the highest accuracy with the highest KGE (>0.77) and lowest RMSE (<~~20mm~~20 mm/month~~), which was comparable to the~~). As expected, the regional ET product MOD16-STM ~~ET product. Most products~~ showed good performance with low RMSE and high KGE (15.84 mm/month and 0.77 when using the ‘*overlap*’ validation samples). This can be attributed to the fact that MOD16-STM ET was calibrated using the flux observations from the TP sites and was estimated based on the regional bias-corrected climate data with better accuracy ~~at the relatively wet sites with dense vegetation (e.g., GT, HBG, ARS, CN-Ha2), judged by relative higher values of KGE and R,~~ than ~~at the relatively dry sites with sparse vegetation or desert (e.g., QOMS, NADORS).~~the global forcing data. These three PM -type model-based products (ETMonitor, PMLV2, MOD16-STM) showed overall better accuracy than other products. The energy balance-based SSEBop ET product ~~exhibited~~had the largest negative bias and lowest KGE for ~~relative~~relatively wet sites and desert sites, but showed good accuracy for some alpine steppe sites with sparse vegetation cover (e.g., SH, YK, NAMORS). Figure 2 also indicates that the ensemble ET datasets (GLASS and SynthesisET) ~~did not exhibit better~~showed poorer accuracy than ~~others~~other ET products, e.g., both with ~~low~~ KGE ~~(both~~ less than 0.6~~)~~ and ~~large~~ negative bias (-13.76 ~ -10.82mm/month), which is most likely related to the ensembled data sources and algorithms. Most products showed better accuracy at the relatively wet sites with dense vegetation cover (e.g., GT, HBG, ARS, CN-Ha2 sites),

带格式的: 字体颜色: 自动设置

带格式的: 字体颜色: 自动设置

带格式的: 字体颜色: 自动设置

带格式的: 字体颜色: 自动设置

带格式的: 字体: 倾斜

带格式的: 字体颜色: 自动设置

as judged by relatively higher values of KGE and R, than that at the relatively dry sites with sparse vegetation cover or desert (e.g., QOMS, NADORS).

Figure 2: Summary of the validation results of high-resolution ET products against flux tower measurements. ~~*AllSite*~~'All' indicates that the validation results are obtained based on different samples depending on the availability of each product, while

~~*VegSite*~~*'Overlap'* represents the validation results are obtained based on same sample numbers (mainly vegetation covered sites ~~during 2001~2018~~) for every product.

3.1.2 Evaluation of ET products against water balance model estimates

Figure 3 and Supplementary Figure S3 ~~show~~showed the comparison ~~between~~of all ET products with the basin-scale water balance ET (ET_{wb}). As ~~anticipated~~expected, the regional ET products ~~(~~MOD16-STM and PMLV2-Tibet~~)~~ showed good ~~accuracy~~agreement with the water balance-based ET of the five river basins described in Section 2.2.2, with KGE of 0.64~0.87 and RMSE of 12.19~15.60 mm/month. Although both MOD16-STM and PMLV2-Tibet were calibrated using the ground flux observations ~~in~~from the TP, their ~~performance differed~~accuracy is different, with ~~MOD16STM~~the MOD16-STM ET ~~showed~~showing a slightly lower KGE, most likely due to its ~~relative~~ underestimation ~~when ET values were~~at high ET levels (Figure 3 and Supplementary Figure S3). ETMonitor and PMLV2 ET also ~~showed~~had high KGE (⩾0.80) and low RMSE (<14mm/month). SynthesisET ~~produced~~had the highest RMSE and BIAS, ~~which~~this is ~~because~~due to the fact that SynthesisET ensembles different data sources ~~during~~in different time periods, resulting in inconsistent time series~~ inconsistency.~~. Among the coarse resolution reanalysis and LSM ET products~~ with coarse resolution~~, TerraClimate, ERA5, and ERA5-Land showed overall good accuracy with KGE⩾0.78 and RMSE≈13 mm/month, while GLDAS-CLSM and GLDAS-VIC ~~exhibited~~showed large errors with RMSE⩾20 mm/month and KGE⩽0.41. CR also showed overall good accuracy in the TP, but had relatively lower KGE in arid basins (e.g., InnerTP), where GLEAM and SSEBop showed relatively higher KGE. ~~Among~~Of all~~ the~~ products, the PMLV2-Tibet and ETMonitor ET products showed the lowest RMSE (<13mm/month) and the highest KGE (0.87) and R (>0.90) when ~~comparing with~~compared with ET_{wb}. The global ET products ~~with above-average accuracy include~~ ETMonitor, PMLV2, GLEAM35a, GLEAM35b, TerraClimate, ERA5, and ERA5Land~~, judged from~~ showed above-average accuracy due to their lower RMSE and higher KGE. When regressed against ET_{wb}, most ET products showed slope values less than one, indicating these ET products ~~tend to~~ underestimate ET in regions or periods with high ET values (Supplementary Figure S3). Among them, ETMonitor, CR, and TerraClimate ET showed slope values close to 1 (larger than 0.9), which highlights their good accuracy in the reference basins.

带格式的: 字体: 10 磅, 字体颜色: 自动设置

带格式的 ...

带格式的 ...

带格式的 ...

带格式的 ...

带格式的 ...

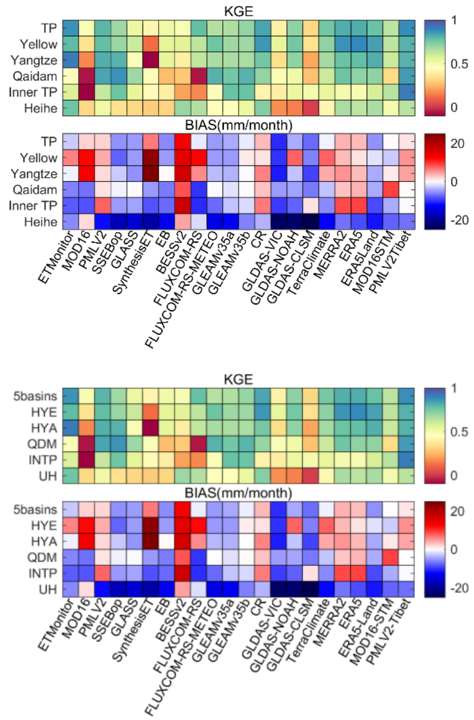

Figure 3: Summary of the ~~validation results~~evaluation of ET products against basin-scale ET based on water balance ~~modelling. TP~~estimates for the headwaters of Yellow basin (HYE), headwaters of Yangtze basin (HYA), upper Heihe basin (UH), Inner TP (INTP) and Qaidam (QDM). '5basins' presents the validation results when data from all five basins were ~~adopted.~~used together.

3.2 Variability of ET across the TP

3.2.1 Spatial ~~variation~~variability in ET across the TP

Figure 4 ~~presents the spatial variation of multi-year averaged annual ET across TP by different products. The~~ shows the mean value of the multi-year average annual ET from the 22 ET products and the standard deviation ~~are also displayed in Figure 4.~~across the TP, and Supplementary Figure S4 documents the spatial variability of multi-year average annual ET across the TP by each product. The annual ET in the river basins over the TP by different products is summarized in Supplementary Table S2. In general, most of the products ~~indicated~~showed pixel-wise ET values ~~lower than 800mm~~below 800 mm/yr and ~~presented~~showed a similar spatial pattern, with high ET values in the eastern part and low ET in the western part of the TP.

带格式的: 字体颜色: 自动设置

带格式的: 字体: 10 磅, 字体颜色: 自动设置

The ~~pixel-wise~~regional ET histogram showed two peaks for some datasets, e.g., ETMonitor, EB, MERRA2. These peaks correspond to the low ET values of non-~~vegetation~~vegetated or sparsely-~~-~~ vegetated regions in the ~~middle~~central and western TP and the high ET values of regions in the eastern TP with dense vegetation and ~~relative~~relatively humid climate. The spatial ~~variations of~~variability, expressed by the standard deviation of different products ~~is also shown in (~~(Figure 4~~, and~~), suggest large differences ~~among~~between different products in the ~~middle~~ central to~~ west~~ western TP~~ can be noticed~~, where ~~some~~most ET products show low ET values~~ (~~, e.g., ET values from ETMonitor, SSEBop, EB, are generally less than ~~200mm~~200 mm/yr~~)~~, while some ET products show much higher ET values~~ (~~, e.g., ET values from BESSv2, ~~CR, and ERA5 reach 400mm/yr~~ERA5, and ERA5-Land reach 400 mm/yr, illustrating their overestimation in the arid regions/basins (Supplementary Table S2).

带格式的: 字体颜色: 自动设置

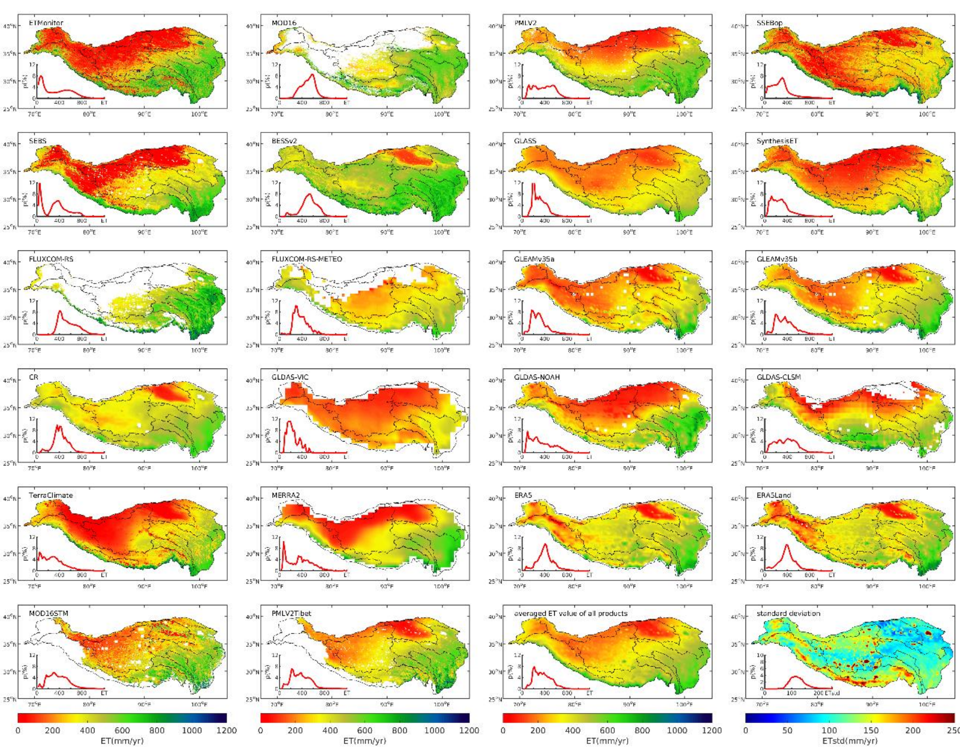

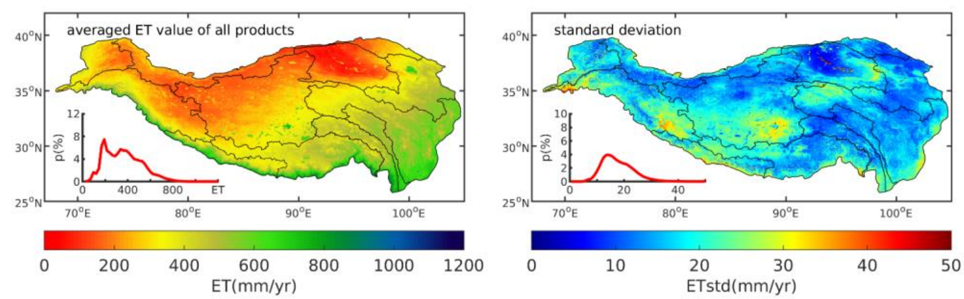

Figure 4: Spatial variation ofMean multi-year average annual ET in Tibetan Plateau by differentfrom the 22 products and the standard deviation across the TP during their overlap period (2003~2013). The inset in each panel shows the histogram of ET values.

Figure 5 summarizes the multiple-year averaged ET in TP and different basins using different productsaverage ET over different products in the TP.. It should be noted that some products only provide ET values for the vegetation-covered regions, e.g., MOD16, FLUXCOM-RS and FLUXCOM-RS-Meteo, and their ET shown here are obtained only based on the available data. Among all the ET products, BESSv2 ET presents highest multiple-year averagedaverage ET value in the TP, while GLDAS-VIC shows the lowest ET values (Figure 5). According to the evaluation results mentioned above, seven ET products (ETMonitor, PMLV2, GLEAMv3.5a, GLEAMv3.5b, TerraClimate, ERA5, and ERA5Land) were found to have continuous spatial coverage and provide accurate estimates, and the median and average annual ET by these products in the TP are 362.21 mm/yr and 350.34 mm/yr, respectively, with a standard deviation of 42.46 mm/yr. Based on the TPHiPr precipitation data (Jiang et al., 2023), the total annual precipitation in the TP is 631 mm/yr, therefore ET accounts for roughly 55(±7)% of the annual total precipitation. The difference among these products also noticeable at the basin scale. The basins with low ET and sparse vegetation cover (e.g., Qaidam, Inner PlateauTP, Hexi Corridor, Tarim, and Amu Darya) exhibithave the largest inter-product uncertainty between products, expressed as the ratio of standard deviation to the averagedmean values (Supplementary Table S1). The uncertaintyS2). Uncertainty is also high in the Indus basin and Brahmaputra basin is also highbasins, most likely due to their complex topography, extreme high elevationaltitude, and large coverageareas of permanent glaciers and snow, which make it difficult to achieveobtain reliable estimates. According to the above-mentioned evaluation results, five ET products (ETMonitor, PMLV2, GLEAMv3.5a, GLEAMv3.5b, TerraClimate) were found to have continuous spatial coverage and provide reliable estimates; the median and average annual ET from these five products in the TP are 339.9 mm/yr and 333.1 mm/yr, respectively, with a standard deviation of 38.3 mm/yr. Based on the TPHiPr precipitation data (Jiang et al., 2023), the total annual precipitation in the TP is 631 mm/yr, so ET accounts for about 52(±7)% of the total annual precipitation. The difference among these products is also noticeable at the basin scale.

带格式的: 字体颜色: 自动设置

带格式的: 字体颜色: 自动设置

带格式的: 字体颜色: 自动设置

带格式的: 字体颜色: 自动设置

带格式的: 字体颜色: 自动设置

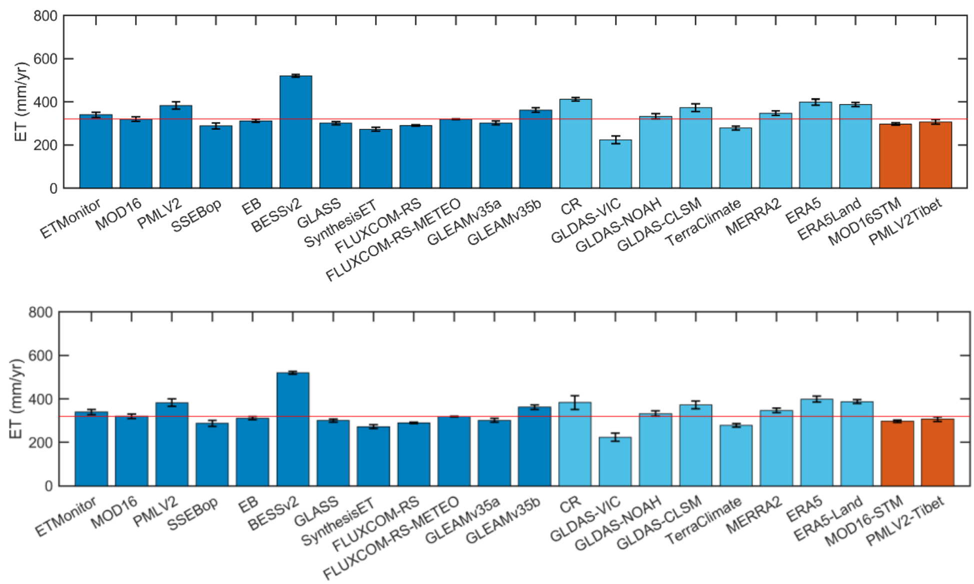

Figure 5: Bar plot of the ~~multiple~~ multi-year (2003~2013) averaged ET ~~in Tibetan Plateau by~~ of different products in the TP. The red horizontal line represents the average ET of all products. The global ET datasets based on satellite remote sensing are in dark blue, the global ET datasets based on land surface models and analysis global ET dataset are in light blue, the regional ET datasets are in red. It should be noted that some products only provide ET values for the vegetation-covered regions, e.g., MOD16, FLUXCOM-RS and FLUXCOM-RS-Meteo, and there are two products (MOD16-STM, PMLV2-Tibet) cannot cover the regions outside of China.

3.2.2 Temporal ~~variations~~variability in ET across the TP

Figure 6 ~~presents~~shows the monthly variation of ET across the TP, while Supplementary Figure ~~S4~~S5 illustrates the ~~difference~~differences between different products. Despite the ~~varying different shapes~~diverse temporal profiles observed, most products indicate that the highest ET occurs in July and August. ET during the monsoon ~~season~~ (June to September) and pre-monsoon ~~season~~seasons (March to May) accounts for 62% (±7%) and 23% (±4%) of the annual total ET, respectively. The remaining 15% of ET occurs during October to next February. ~~As a comparison~~In summary, 66% and 22% of the annual ~~total~~ precipitation occurs during the monsoon and pre-monsoon seasons~~, while~~ respectively, with the remaining 12% occurring during the rest of the year. The monthly patterns of ET ~~variations~~variability are similar ~~across~~in all basins, with differences in magnitude. The proportion of ET during the monsoon season is higher in the dry basins, e.g., 69% in Hexi Corridor and 68 % in Qaidam, compared to the wet basins, e.g., 53% in the Ganges and 58% in the Brahmaputra.

带格式的: 段落间距段前: 18 磅, 段后: 6 磅

带格式的: 字体颜色: 自动设置

带格式的: 字体颜色: 自动设置

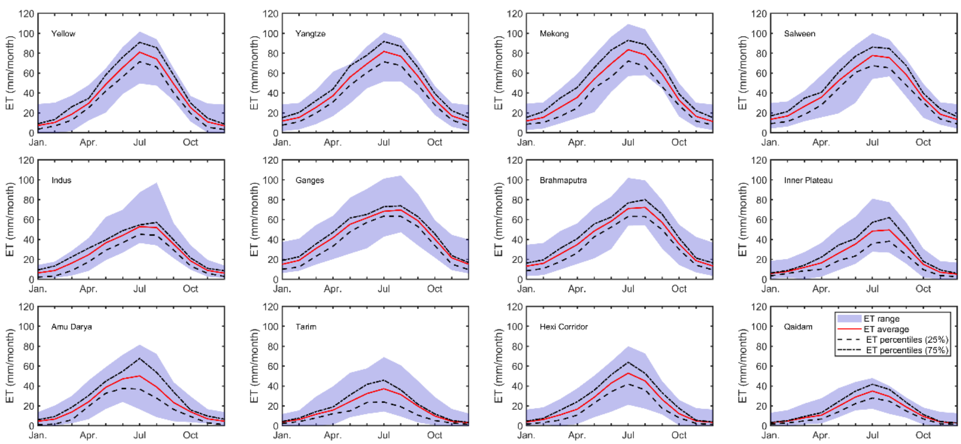

Figure 6: Seasonal ~~variation~~evolution of ET in different basins in ~~Tibetan Plateau.~~the TP. Data shown are monthly averaged ET ~~value of~~values during 2003~2013.

Figure 7 ~~presents~~shows the ~~yearly variation~~time series of annual ET ~~across~~ spatially averaged over the TP for different products. Large deviations were observed among the products, with ~~CR and ERA5~~BESSv2 having the ~~largest~~highest value of ~~averaged~~ spatial-average annual ET ~~while~~and the GLDAS-VIC ~~has~~having the lowest. The trend of annual ET varies with different products and their temporal coverage (Figure 7 and Supplementary Figure ~~S5~~S6). The results suggest a general, significant, increasing trend of ET since the 1980s~~.~~ (most products with $p<0.05$). Since 2000, the annual ET has ~~showed~~shown both positive and negative trends depending on the product. Most products showed a significant increasing trend~~,~~ ($p<0.05$), and the median ET of all products increased at a rate of 1.70 mm/yr from 2000 to 2020 in TP~~.~~ ($p<0.05$). The SynthesisET showed the largest significant negative trend ~~due to its temporal inconsistency.~~. At the basin scale, the difference in annual trends ~~among~~between different products is also clearly illustrated (Supplementary Figure ~~S5~~S6). Most basins ~~are experiencing~~ showed ~~an~~ significant increasing trend of ET, ~~particularly~~especially the Yellow, Yangtze, Mekong, Tarim, Hexi Corridor, Tarim, and Qaidam basins, where most products had a positive ET trend. The median ~~values of~~ ET trend ~~are~~is either negative or close to zero in the Ganges, Brahmaputra, Amu Darya, and Inner ~~Plateau, which~~TP basins, probably ~~indicates~~indicating a decreasing or non-monotonic trend for these basins.

带格式的: 字体颜色: 自动设置

带格式的: 字体颜色: 自动设置

带格式的: 字体颜色: 自动设置

带格式的: 字体颜色: 自动设置

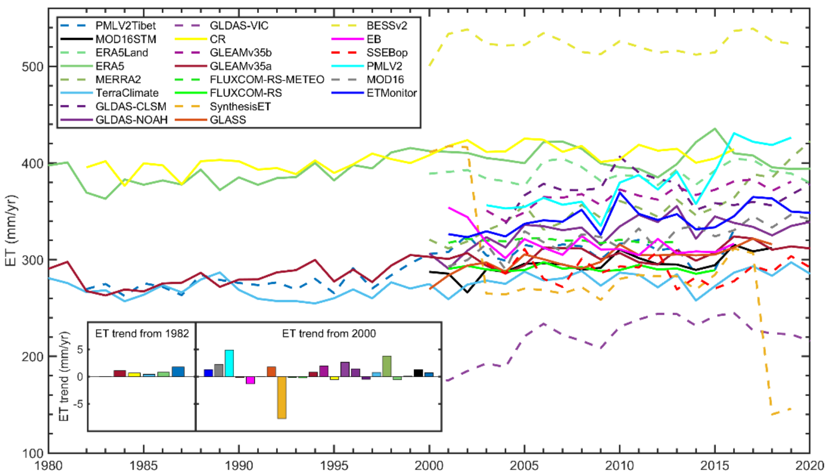

PMLV2Tibet
MOD16STM
ERA5Land
ERA5
MERRA2
TerraClimate
GLDAS-CLSM
GLDAS-NOAH
GLDAS-VIC
CR
GLEAMv35b
GLEAMv35a
FLUXCOM-RS-METEO
FLUXCOM-RS
SynthesisET
GLASS
BESSv2
EB
SSEBop
PMLV2
MOD16
ETMonitor
ET (mm/yr)
ET trend from 1982
ET trend from 2000
ET trend (mm/yr)

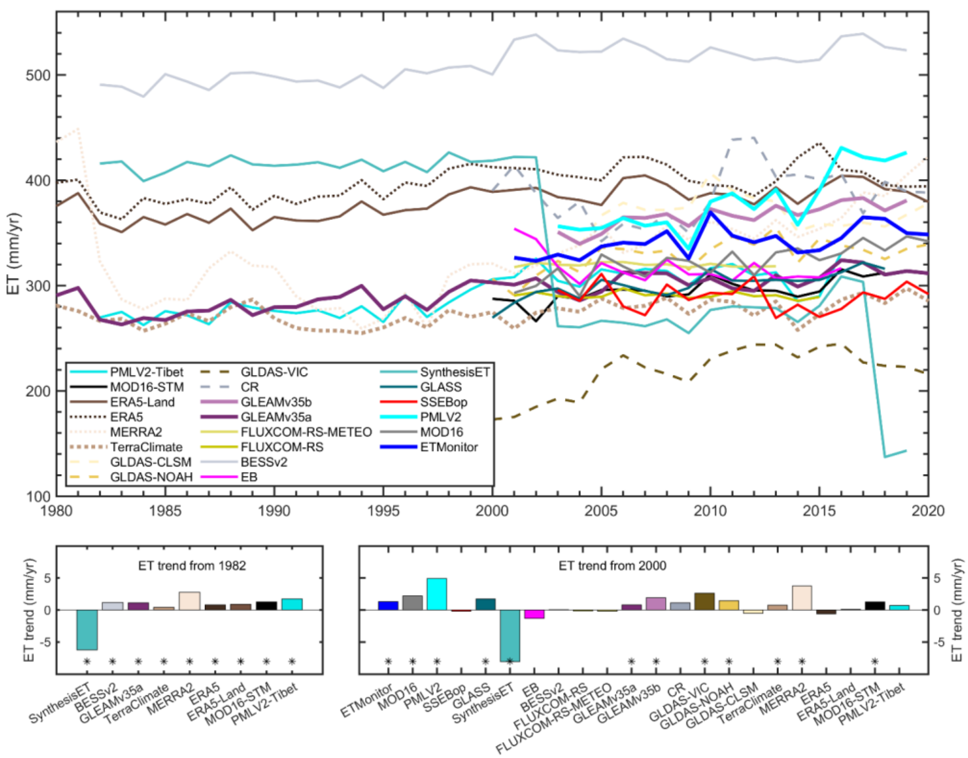

Figure 7: ~~Yearly variation~~Time series of annual ET ~~in Tibetan Plateau~~ by different products in the TP. The inset panel shows the annual ET trend by different products. *: trend with significance level (*p*<0.05). In the upper panel, the reanalysis data are shown by a dotted line, and the land surface model-based data are shown by a dashed line.

3.~~2.~~3 ET components

~~Among these products, there are nine that provide~~We also compared the main ET components~~ of ET~~ (, i.e., Ec, Es, and Ei~~),~~ from nine products, including ETMonitor, PMLV2, ~~MOD16STM~~MOD16-STM, GLEAMv35a, GLEAMv35b, GLDAS-VIC, GLDAS-NOAH, GLDAS-CLSM, and MERRA2. It is important to note that there is no independent reference data available ~~for~~to validate the ET components, and each model has a ~~distinct~~different way of estimating these components. Even when the total ET is consistent across ~~various~~different products, the individual components can differ significantly (Figure 8 and Supplementary Figure ~~S6~~S7). All products show higher Ec and Ei values in the eastern TP and lower values in the ~~middle~~central and western TP (Supplementary Figure S7). This pattern follows the spatial distribution of environmental factors (e.g., LAI

带格式的: 标题 2, 段落间距段前: 24 磅, 段后: 6 磅, 行距: 单倍行距

带格式的: 字体颜色: 自动设置

带格式的: 字体颜色: 自动设置

and precipitation), i.e.~~.~~, regions with high ET values are mostly covered by forest and alpine meadow with higher precipitation, ~~while~~whereas regions with low ET values are dominated by ~~where~~ sparse vegetation (alpine steppe and desert steppe) with lower precipitation. Large deviations in Es values were observed~~ in Es values~~, with several products ~~exhibiting~~showing high Es values in the eastern TP, e.g., MERRA2, GLDAS-CLSM, ETMonitor, and ~~MOD16STM~~MOD16-STM, while some products showed extremely low Es values, e.g., GLEAMv35a, GLEAMv35b, and GLDAS-VIC.

Figure 8 ~~presents~~shows the false color composite maps of the relative magnitude of transpiration (Ec), soil evaporation (Es), and interception (Ei) ~~by~~from different products, with Red (Es is largest), Green (Ei is largest), Blue (Ec is largest). In the false color composite maps, the red (green, blue) color means that Es (Ei, Ec) contributes most to total ET. ~~Clear~~There are clear differences ~~exist among~~between different products. Most products generally ~~suggest~~indicate that Es ~~contributed most~~is the major contributor to ~~the~~ total ET~~.~~ (Figure 8, pie diagram). In contrast, three products (GLEAMv35a, GLEAMv35b, and GLDAS-VIC) show that plant transpiration is the ~~primary~~main contributor to total ET~~, mostly~~ (Figure 8, pie diagram), most likely ~~caused by their extreme~~due to the extremely low Es values in the eastern TP ~~by these three products~~ (Supplementary Figure ~~S6~~S7). The averaged Es/ET values range from 18% ~~by~~in GLDAS-VIC to 84% ~~by MOD16STM~~in MOD16-STM, with a median value of 50%. ~~The averaged~~Averaged Ec/ET values range from 11% ~~by~~in GLDAS-CLSM to 58% ~~by~~in GLEAMv35a, with a median value of 30%. Most products generally showed low Ei/ET values with a median value of 5%, while GLDAS-VIC and GLDAS-NOAH ~~exhibit~~show the highest Ei/ET ~~value~~values (20% ~ 36%). Overall, the ET partitioning ratio in ETMonitor is the closest one to the median value of all products.

带格式的: 字体颜色: 自动设置

带格式的: 字体颜色: 自动设置

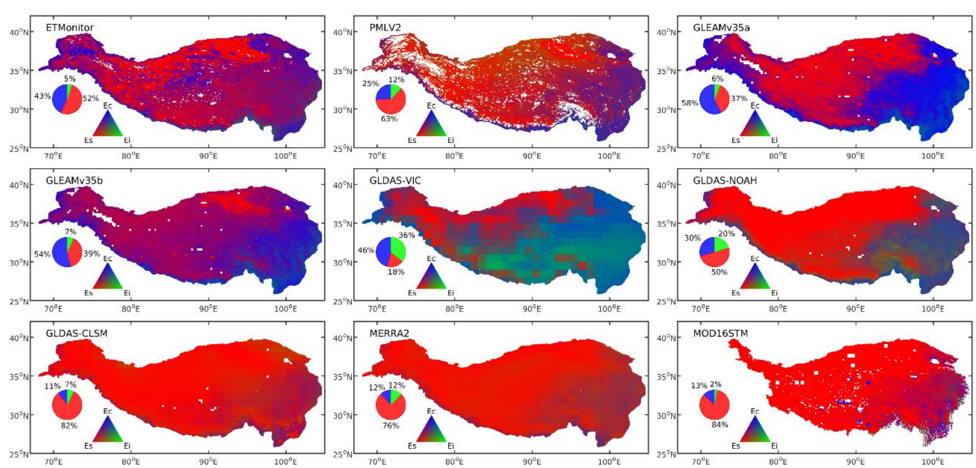

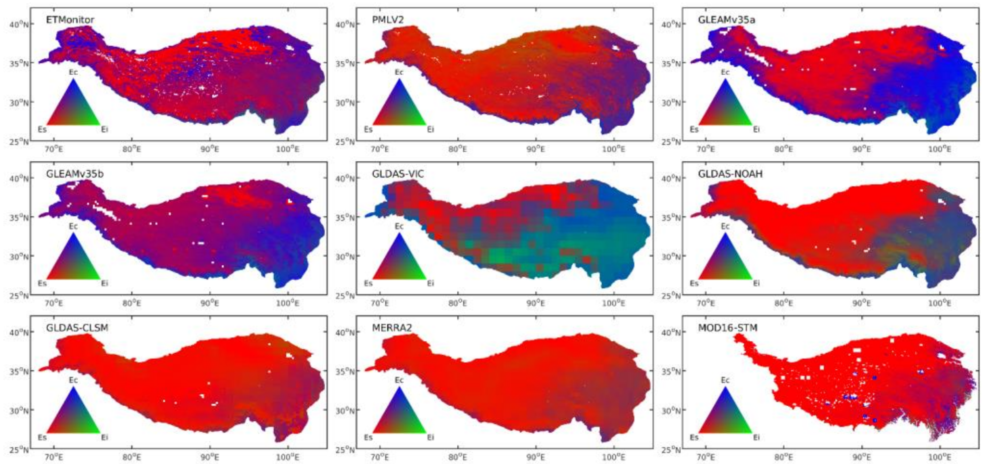

Figure 8: False color composite maps to visualize the relative magnitudes of the transpiration (Ec), soil evaporation (Es), and interception (Ei) contribution to total ET according to different products.

In addition, two other components of water vapour flux are considered separately: evaporation from open water bodies (Ew) and sublimation from snow/ice-covered surfaces (Ess). There are three products providing open water evaporation, including ETMonitor, GLEAMv35a and GLEAMv35b (Figure 9, upper panel), and five products providing snow/ice sublimation, including ETMonitor, GLEAMv35a, GLEAMv35b, GLDAS-CLSM, and MERRA2 (Figure 9~~).~~, middle and lower panels). For open water evaporation, three products provide comparable Ew results with average Ew/ET from 3.45% to 4.10%. According to Wang et al. (2020), the total water evaporation is about 29.4 ± 1.2 km^3/yr (≈1111.5 mm/yr) from the 75 lakes in the TP with total area of 26,450 km^2 (accounting for approximately 56.9% of the total lake area in the whole TP), and the total lake evaporation (51.7 ± 2.1 km^3/yr) for all plateau lakes. The total open water evaporation amount from ETMonitor gives a value of 945.3mm/yr for the permanent water surface over the TP. The total water area is 1.29×10^6 km^2 in the TP when seasonal water bodies are taken into account, which is much larger than the permanent water surface. ETMonitor takes into account the seasonality of water surface areas when estimate ET, and the multi-year mean total annual water evaporation in the TP estimated by the ETMonitor is about at 44.4 km^3/yr, which is lower than that given by Wang et al. (2020). For snow/ice cover surface~~ sublimation~~, GLDAS-CLSM provided the overall highest ratio of sublimation (Ess~~/~~) to total ET ~~value~~(i.e. Ess/ET) with a regional ~~average~~mean of 7.79~~%~~%, and GLEAMv35a provided the overall lowest Ess/ET value with a regional ~~average~~ mean of 1.20%. This difference is mainly caused by large differences ~~of~~in Ess ~~among~~between different products in the southern TP, e.g., in the Indus, Ganges and Brahmaputra watersheds, where Ess is not well captured by GLEAM. The sublimation (Ess) estimated by the ETMonitor~~'s Ess~~ falls in the middle of these ~~extremes~~ET products, with a regional average of 4.3%.

带格式的: 字体颜色: 自动设置

带格式的: 字体颜色: 自动设置

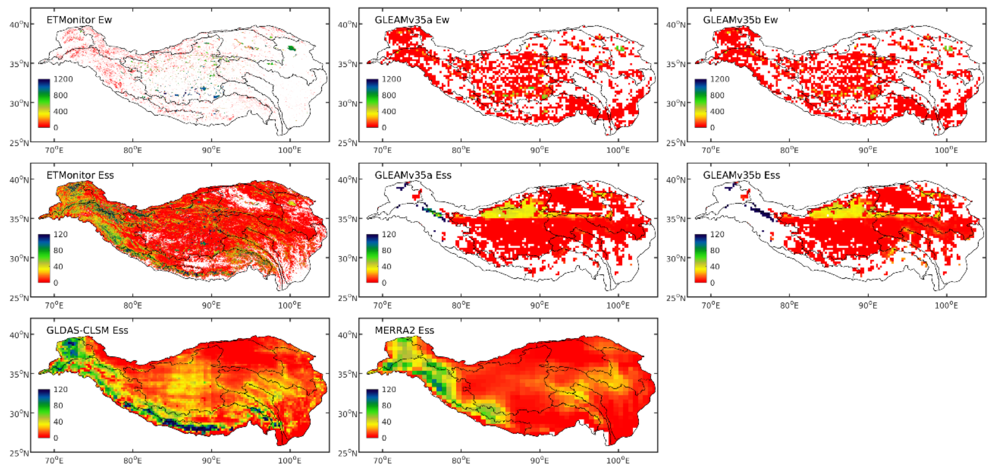

Figure 9: Spatial variability of open water evaporation (Ew) and snow/ice sublimation (Ess) in ~~Tibetan Plateau~~the TP by different products.

~~3.3 Response of annual ET to the main governing environmental factors~~

~~Figure 10 shows the pixel-wise median R values of all ET products with precipitation, Rn, and LAI. A negative R value was obtained when ET exhibited an opposite annual trend to the regulation effect. ET and precipitation showed high positive R in the water-limited middle and northern part of TP (e.g., Inner Plateau, Qaidam, Hexi Corrida, Yellow), while they showed negative R in the southeast part of TP (e.g., Yangtze, Mekong, Salween, Brahmaputra) with high precipitation and limited energy due to cloudiness. ET had positive correlation with Rn in the northern part of TP (the water-limited regions, e.g., Yellow, Qaidam, Hexi Corrida), however with smaller R than with precipitation. ET and Rn also showed positive correlation in the eastern part of TP (e.g., Yangtze, Mekong, Salween, Brahmaputra), indicating that energy plays a more important role than water in regulating the variability of ET in these regions. Conversely, ET and Rn showed negative correlation in the middle part of TP (e.g., Inner Plateau) since this region is mainly water-limited. The correlation between ET and LAI is generally weak, however large positive R values could be found in the north and east part of TP (especially in the Yellow, Hexi Corride, and Qaidam) and occasionally in other areas. It should be noticed that plants tend to grow more (higher LAI) with more water available in the water-limited regions (e.g., Inner TP), and higher correlation between ET and LAI in these regions may also be associated with the governing effect of water. In the energy-limited regions, e.g., Mekong and Salween, higher LAI may result in higher Rn due to the generally lower albedo of plant compared to soil, which reduces the effect of Rn.~~

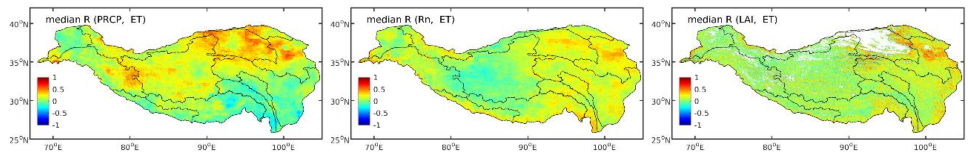

Figure 10: The spatial variation of the median correlation coefficient (R) of ET with precipitation, Rn, and LAI.

Supplementary Figure S7 presents the variables that showed the highest absolute R, with red (green, blue) colors means that Rn (LAI, precipitation) has a highest temporal correlation. This allows for an easy visualization of the most important factors governing ET according to different products. The differences in R values are closely related to the biophysical nature of each algorithm, and are mostly likely associated with the algorithms and the drivers. For instance, GLEAM products utilize surface soil moisture data as input and simulate root zone soil moisture relied on precipitation to account for the impact of available surface water on ET, and the estimated ET were strongly correlated with precipitation, especially in the Inner Plateau region. The difference caused by the drivers are also emphasized, especially when comparing GLEAMv35a and GLEAMv35b, which were produced based on same algorithms but different drivers (Mentens et al., 2017).

4. DiscussionsDiscussion

To understand the regional and global climate change, as well as regional ecohydrological processes in the TP, it requires knowledge of the changes in ET over time and space. This is required. In this study evaluated, 22 ET products were evaluated using various methods, i.e.,g., comparing ET products with ground EC eddy covariance observations and basin-scale water balance estimationsestimates, assessing the spatiotemporal variability of ET and its components, and exploring the response of ET in TP to environmental factors, to assess the performance of ET products and clarify the ET amount and , spatiotemporal variability and trends of ET in the TP. After thesethis comprehensive evaluation and analysis, we have gained a clear understanding of the water vapour released byfrom the TP. AdditionallyIn addition, we noticefind that the evaluation results are highly relevant to better understand the performance of ET modelmodels and the consideredunderlying vaporization processes, and providethus providing suggestions for further implicationsimprovements in the ET estimation for TP. Among the evaluated ET products, there are 14 products that primarily use remote sensing products, including 2 products (SSEBop and EB) based on land surface temperature (LST), 8 products (ETMonitor, MOD16, MOD16-STM, PMLV2, PMLV2-Tibet, GLEAMv35a, GLEAMv35b, BESSv2) based on PM-types models (including Penman-Monteith equation, Priestley-Taylor equation, Shuttleworth-Wallace equation), 4 products (FLUXCOM-RS, FLUXCOM-RS-METEO, GLASS, SynthesisET) based on data-driven methods.the TP.

带格式的: 字体颜色: 自动设置
带格式的: 字体颜色: 自动设置

4.1 Relevance of ~~validation~~evaluation results ~~with~~ towards a better understanding of the vaporization processes

~~4.1.1 Processes captured by tower-based observation using~~ The *in-situ* observations with an eddy covariance system

~~The *in-situ* observation by eddy covariance system is~~are recognized as the standard method for monitoring energy and mass fluxes to validate high-resolution ET (Baldocchi, 2020). ~~The~~ In addition, the ET products were compared with the basin-scale water balance estimates ET_{wb}. ET_{wb} is obtained at the basin scale (several hundred km^2), which is much larger than the footprint of flux tower observations (approximately km^2, depending on meteorological conditions). Given the relatively sparse distribution and small footprint of the flux-tower-based eddy covariance system observations, the water balance method can serve as a useful complementary reference for ET estimates. This is especially true for the coarse-resolution ET, which has a much larger spatial footprints than eddy covariance observations.

带格式的: 字体颜色: 自动设置

In this study, these two methods gave generally consistent results when evaluating the high-resolution ET. When judged by the KGE of site-scale estimates, the accuracy of the high-resolution ET products can be ranked as follows: PMLV2 > ETMonitor > MOD16-STM > GLASS > MOD16 > SynthesisET > SSEBop. When judged by the KGE of basin-scale validation, the accuracy of the high-resolution ET products can be ranked as: ETMonitor > PMLV2 > MOD16STM > SSEBop > GLASS > MOD16 > SynthesisET. Although both indicate that ETMonitor, PMLV2, and MOD16STM are the most accurate and the remaining four are less accurate among the high-resolution ET products, some differences in the ranking of the ET products can be observed. This is probably related to the processes captured by the 'ground-truth' data at different scale used in the two evaluation methods. An eddy covariance observation represents the net water vapour flux integrated across different processes at given point (e.g., plant transpiration in the dense vegetation regions, snow sublimation ~~during the~~in dry snow cover ~~periods~~regions, evaporation of canopy-intercepted water when the canopy is wet due to intercepted rainfall). ~~The~~In addition, the observed vaporization process ~~observed by the eddy covariance system~~ depends on the land surface ~~condition~~conditions at the observation sites during particular times, which may vary seasonally and ~~yearly~~annually due to factors such as snow/ice, intercepted water, and vegetation. The estimated basin-scale ET by water balance (ET_{wb}) was essentially the residual of the observed water balance terms, which is assumed to be the net liquid water flux loss to the atmosphere at the basin scale. Compared to the site-scale observation, the basin-scale ET_{wb} can capture the effect of land cover dynamic on the ET within the basin. For example, the mean water level of lakes in TP increased by 0.20 m/yr from 2000 to 2009, and the lake water mass increased significantly (Zhang et al., 2013), which caused higher ET in the TP because water evaporation is generally higher than other land cover types. However, ~~many~~most ET products (e.g., MOD16~~ and~~, PMLV2, etc) assume ~~a~~ constant land surface ~~condition~~conditions throughout the year or multiple years, which ~~indicate~~means that they cannot capture the temporal transitions of ~~these~~the vaporization process associated with changes in land cover. In contrast, ETMonitor adjusts the daily land cover ~~inputted to the algorithm~~ based on ~~seasonal~~dynamic land cover ~~condition (~~conditions, including water bodies cover and snow/ice cover~~)~~, which ~~enable~~allows it to ~~partly~~ reflect the impact of seasonal and annual open water ~~cover~~extent and snow/ice cover on total ET (Zheng et al., 2022). This probably explains in part why ETMonitor performs slightly better than PMLV2 when validated by basin-scale water balance methods, while they are comparable when validated by *in-situ* observations.

带格式的: 字体颜色: 自动设置

~~Meanwhile, eddy~~Eddy covariance ~~system observation includes~~observations capture condensation when negative latent heat flux (i.e. ET) occurs. Remote sensing-based ET products mainly focus on positive ET (positive upward latent heat flux) and omit processes such as condensation. For example, in the MOD16 ET product algorithm, net radiation (Rn ~~was mandatory~~) is constrained to positive values (Rn ~~was~~is set to 0 if Rn<0) indicating that negative ET is not allowed. Negative ET (e.g., condensation) ~~may~~can also occur when VPD is negative. Depending on whether negative Rn or negative VPD is allowed, the considered water phase changes ~~differs,~~are different and ~~it surely~~this will ~~impact~~certainly affect the ~~performance~~accuracy of the ET products.

~~**4.1.2 Validation results based on basin-scale water balance method**~~

The ~~validation results~~ evaluation using the basin water balance method ~~show generally consistent results and~~gave slightly ~~superior evaluation~~ higher metrics compared to the flux tower ~~validation~~ results. This may be attributed to the ~~representation~~ disparity in spatial resolution between the flux tower measurements and the basin-scale ET_{wb} ~~estimate. ET_{wb} is obtained at the basin scale (several hundred km^2), which is much larger than the footprint of flux tower observations (roughly km^2 depending on meteorological conditions).~~estimates. Basin-scale ET_{wb} may offset the positive and negative biases within the basin, resulting in better evaluation metrics.~~ Considering the relative sparse distribution and small footprint of the flux-tower based eddy covariance system observation, the water balance method can serve as a useful complementary method for validating ET, which is especially true for the coarse-resolution ET that have much large spatial representation than eddy covariance system observations.~~ (Liu et al., 2023). However, ~~it should also acknowledge~~ the uncertainties in the water balance method as ground-truth data should also be acknowledged. This method is based on the validity of several assumptions (e.g., negligible subsurface leakage to adjacent basins) and the reliability of data on precipitation, runoff, and water storage (Mao et al., 2016). In ~~the~~ cold regions ~~like~~such as the TP, where glaciers and snow have a substantial ~~influence~~impact on the water balance, meltwater should also be considered (Wang et al., 2022).

带格式的: 字体颜色: 自动设置

带格式的: 字体颜色: 自动设置

4.2 Implications for ~~ET~~the estimation of ET in ~~Tibetan Plateau~~the TP

4.2.1 ET estimation using PM-type ~~model~~models

This study found that ET products generated using ~~the~~ PM-type ~~model demonstrated superior accuracy compared to~~models were more accurate than other models. In particular, ETMonitor and PMLV2 ~~showed the highest accuracy in TP compared to~~were the most accurate when evaluated by both *in-situ* flux observations and estimates of ET based on the basin-scale water balance~~ estimated ET.~~. This is consistent with the ~~judgment~~conventional wisdom that ~~LST~~energy balance-based ET models are ~~suited~~suitable for water-limited conditions in bare and partially vegetated areas, while PM-type ET models are more effective for both energy-limited and water-limited conditions in vegetated areas (Chen and Liu, 2020). An exception was found for MOD16, which ~~exhibited~~had below-average accuracy overall, ~~however~~but its ~~regional~~regionally improved version (MOD16-STM) ~~demonstrated~~gave significantly more accurate estimates of ET after regional parameter calibration and improvement of the soil evaporation module ~~enhancement~~ (Yuan et al., 2021). The reason for this is that MOD16 is only ~~applies~~applicable to limited areas and seasons of the TP due to its ~~incomplete~~unfavourable parameterization, which ~~fails to address the ET variation~~does not account for conditions in the ~~middle~~central to western TP ~~because it lacks~~due to the lack of estimation of bare soil and open water evaporation.

This study also highlights the potential for improving ~~of parameterization or~~model parameters ~~for estimating~~to estimate ET using PM-based ~~model~~models, e.g., by incorporating soil moisture ~~as~~to compute a water ~~available~~ stress ~~or indicators~~indicator, by integrating the water balance simulation and data assimilation, or by coupling ~~with~~ the water and carbon ~~cycle in simulating~~cycles to estimate ET. We found that PM-type models ~~that incorporated~~incorporating soil moisture to ~~detect~~parameterize water stress ~~produced~~gave very good results. For instance, to ~~enhance~~improve the accuracy of ~~estimated~~ ET estimate, ETMonitor utilized high-resolution soil moisture data to refine the ~~soil resistance and canopy resistance~~ parameterizations ~~for plant transpiration and~~of soil and canopy surface resistances to estimate soil evaporation~~,~~ and ~~calibrated the most sensitive parameters based on ground observation~~ plant transpiration (Hu and Jia, 2015; Zheng et al., 2022). GLEAM ~~assimilated~~assimilates surface soil moisture to ~~derive the~~estimate water availability ~~at~~in the root zone, and ~~applied~~applies it to determine the water stress (Miralles et al., 2011), which also ~~showed good accuracy~~gave accurate estimates of ET in the TP. Coupling ~~ET estimation with~~ the water and carbon ~~cycle~~cycles can also be helpful for better estimates of ET, e.g., PMLV2 adopted water-carbon cycle coupling to ~~aid~~estimate ET ~~estimation~~ (Zhang et al., 2019), since canopy conductance controls both transpiration and photosynthesis. The regional ~~adaption~~adaptation of ~~parameterization~~parameterizations and better ~~driven forces~~forcing are also ~~appreciated, and their benefit were clearly illustrated~~beneficial, as shown in this study ~~that~~, where MOD16-STM and PMLV2-Tibet products showed better agreement with reference values than MOD16 and PMLV2. Furthermore, ~~the~~ PM-type model-based ET products (especially those based on duel-source or multi-source models) can provide different ET components, benefiting from ~~its inherent advantage in expressing the biological and non-biological~~the more realistic representation of biotic and abiotic processes.

4.2.2 ET estimation using LST-based model

Although the absolute accuracy of ~~LST~~the energy balance-based EB and SSEBop products may be lower than that of the ET products ~~by~~from the optimized PM-types models, they have some advantages, ~~e.g.,~~such as the close coupling of energy balance ~~through~~with sensible heat flux~~,~~ and the good ~~capability of representing~~ability to present the spatial ~~variations~~variability of ET, especially for the high-resolution dataset. Previous ~~study criticized~~studies pointed out that the LST-based models fail to produce temporally and spatially continuous ET fields under variable cloud conditions~~, which~~ . The continuity of LST was significantly improved recently through ~~the~~ temporal upscaling technologies~~, advanced satellite observations (Ryu et al., 2012;~~

带格式的: 字体颜色: 自动设置

带格式的: 字体颜色: 自动设置

带格式的: 字体颜色: 自动设置

带格式的: 字体颜色: 自动设置

带格式的: 字体颜色: 自动设置

~~Tang et al., 2017; Zhong et al., 2019).~~ , which may further benefit the ET estimation. The relatively good ~~performance~~accuracy of SSEBop at some sites (e.g., SH, YK, NAMORS) in this study also demonstrates the potential of LST-based models to achieve ~~accurate~~estimate ET ~~estimation at~~accurately in arid ~~sparse~~ and sparsely vegetated regions.

4.2.3 Uncertainty propagation in data-driven ensemble ET products

The accuracy of ET products based on data-driven models ~~performed diverse~~has been quite variable in the TP. GLASS and SynthesisET ~~were~~are both ~~obtained based on~~ ensemble ~~different~~ ET products, with GLASS ~~adopting~~employing Bayesian averaging ~~method~~ and SynthesisET using a ranking-based method (Yao et al., 2014; Elnashar et al., 2021). However, these two products ~~exhibited~~showed significant differences, with SynthesisET showing much larger errors (Figure 3 and Figure 4). This finding on SynthesisET ~~differ~~differs significantly from a previous study that validated ET product at the global scale (Liu et al., 2023), which claimed that SynthesisET was the best product when applied in its time span based on accuracy indicators (e.g., RMSE) by comparing to *in-situ* observations and water-balance ~~estimation~~estimates. After screening the time series of SynthesisET, we found significant temporal ~~inconsistency,~~inconsistencies (much higher ET values before 2000 than after, which is also shown in Figure 7), mainly caused by its synthesis method. SynthesisET ~~incorporated~~ensembled two or three high-~~ranked~~ranking ET datasets ~~in~~at each time step according to the evaluation metrics~~, i.e.,~~. The use of different products ~~were adopted~~ for different time periods, without correcting for the ~~inherent discrepancy of~~ differences in different products, ~~which may be improved by~~eliminates the possibility of improving the quality of a data product through an advanced ensemble method or critical ~~inputs~~ selection of inputs (Wang et al., 2021). Therefore, to ensure a more reliable and comprehensive ~~evaluation~~assessment, we ~~suggest addressing the evaluation in terms of~~ propose to analyse the spatial and temporal ~~variation. Additionally, when conducting further data ensemble studies, it is important to properly consider the temporal inconsistency of different products~~variability of ET as in Section 3.2 of this study.

Data-driven methods, especially ~~the~~ machine ~~learning~~ or deep learning methods, are increasingly applied in ~~earth science~~the geosciences to extract land surface ~~parameters~~information (Karpatne et al., 2017). The FLUXCOM product integrates the ET results upscaled from *in-situ* observations using various machine learning models (Jung et al., 2019). The FLUXCOM-RS-METEO product, which is obtained using both meteorological datasets and remote sensing datasets as ~~driven forces~~drivers, is also found to have ~~with comparable~~a good accuracy in TP. However, the FLUXCOM-RS product, which ~~differ~~differs from FLUXCOM-RS-METEO~~ that FLUXCOM-RS product is obtained without using meteorological datasets as driven forces~~, performs poorly in the TP according to the ~~validation in~~findings of this study, indicating the importance of meteorological variables in estimating ET.

4.2.4 LSM and ~~analysis~~reanalysis ET products

We also compared ~~various~~several ET products ~~by~~from LSM and climate ~~analysis~~reanalysis, including GLDAS-Noah, GLDAS-VIC, GLDAS-CLSM, CR, TerraClimate, ERA5, ERA5Land, and MERRA2. Although these products generally have

带格式的: 字体颜色: 自动设置
带格式的: 字体颜色: 自动设置
带格式的: 字体颜色: 自动设置
带格式的: 字体颜色: 自动设置
带格式的: 字体颜色: 自动设置
带格式的: 字体颜色: 自动设置
带格式的: 字体: 倾斜
带格式的: 字体颜色: 自动设置
带格式的: 字体颜色: 自动设置
带格式的: 字体颜色: 自动设置
带格式的: 字体颜色: 自动设置

low spatial resolution (0.1°~1.0°), they have a long~~-term~~ temporal coverage, making them more suitable for climate ~~analysis~~studies. Among them, TerraClimate, CR, ERA5, and ERA5~~-~~Land showed overall good accuracy when compared ~~with~~to ET_{wb}, while GLDAS products ~~yield~~had a relatively low accuracy. The ~~performance~~poorer accuracy of GLDAS ET datasets ~~are~~is mainly caused ~~with~~by the ~~driven forces~~forcing data and parameter settings, which need significant improvement when ~~applying in~~ applied to the TP (X. Li et al., 2019). In the ~~middle~~central and western regions of the TP, where the surface vegetation cover is sparse and the climate is arid or semi-arid with ~~very~~ low precipitation (roughly ~~300mm~~300 mm/yr or less), CR, ERA5, and ERA5~~-~~Land produce higher ET values than other products~~ which exhibit lower ET values.~~. The high ET values of ERA5 and ERA5~~-~~Land are most likely due to the ~~overestimated~~ overestimation of precipitation in the TP by ERA5 (Jiao et al., 2021; Xie et al., 2022), which ~~will also lead~~leads to the overestimation of both ET and runoff (Sun et al., 2021). Previous studies have reported ~~the~~ relatively high ET values ~~by~~from CR methods in ~~middle~~the central and western TP (Yang et al., 2020) and Arctic basins (Ma et al., 2021), which can be partly explained by the uncertainty of the ~~driven forces partly~~forcing (Ma et al~~.,~~., 2021) and by the applicability of CR in cold regions ~~with complex energy processes~~during non-thawing periods (Yang et al., 2021). A basic assumption of CR is that the energy difference between ~~apparent~~ potential ET (ET_P) and the ET under wet ~~environment ET~~conditions has a linear or nonlinear relationship with the energy difference between ET_P and actual ET when water is limited~~, which~~. This relationship fails during periods of soil freezing and thawing~~ periods,~~ when the available energy is mainly used for the phase change of ice-water ~~and sublimation~~ (with~~ much~~ higher latent heat) (Yang et al., 2021). Furthermore, CR also assumes that the changes in land surface properties can be accurately and promptly ~~detected~~estimated from changes in atmospheric conditions, neglecting regional or large-scale advection, which makes it ~~unapplicable~~inapplicable in heterogeneous ~~surfaces~~areas (Morton, 1983; Han and Tian~~.,~~, 2020; Crago et al., 2021).

4.2.4 Suggestions for further ET estimations in TP

Several aspects could be addressed to improve the ET estimation in the TP~~, several aspects can be addressed. Current~~. The current ET models could be improved by integrating different models and processes, ~~e.g.,~~such as combination of LST-based models and conductance-based PM-types models (Chen and Liu~~.,~~, 2020) or data-driven algorithms (Zhao et al., 2019; Shang et al., 2023), ~~combination of~~ combining ET processes with carbon cycle and hydrological processes (Zhang et al., 2019; Abatzoglou et al., 2018). ~~Combining the~~ The appropriate combination of PM-type models and machine learning algorithms ~~in a proper way can inherit both advantages~~could benefit from both and result in a more powerful model for ET estimation (Koppa et al., 2022~~), and recent~~). Recent studies have highlighted the improved accuracy of the hybrid model by ~~incorporating the~~estimating the canopy conductance using machine learning methods ~~estimated canopy conductance with~~and applying PM-~~types equation for ET estimation~~type models (Zhao et al., 2019; Shang et al., 2023), which is ~~another~~ direction ~~for further~~towards better estimates of ET ~~estimation~~ in the TP. ~~Meanwhile, a main~~A major challenge in improving ~~the ET algorithm~~ or ~~validating the estimation~~evaluating ET algorithms is the scarcity of ~~the~~ ground measurements, which ~~highlight~~highlights the need for the long-term comprehensive ~~observations~~observation network in the TP (Ma et al., 2020; Zhang et al~~.,~~., 2021). Furthermore, to improve the accuracy of the estimated ET, it is recommended to ~~employ~~use regionally optimized ~~driving forces~~forcing data, e.g., climate reanalysis ~~dataset that considers~~ data, which account for the specific climate of the TP with higher accuracy and resolution (He et al., 2020).

带格式的: 字体颜色: 自动设置

4.3 Differences in ET components

Previous studies have mostly focused on the total net vapour flux, e.g., magnitude, spatial variability, temporal trend, etc., while the ET components have not been fully investigated. The partitioning of ET into its components, such as soil evaporation (Es) and plant transpiration (Ec), can vary significantly between different datasets. These components reflect the different water phase transitions and vapour flow processes that are regulated by different factors, i.e. vapour flow within plant leaves is mainly controlled by the stomatal behaviour in response to environmental conditions, soil evaporation is controlled by soil structure and water content, the rainfall interception is determined by canopy morphology and rainfall intensity, and vapour transport after sublimation is determined by near-surface boundary layer conditions and the higher latent heat of sublimation. A recent study shows that the contributions of Es, Ec, and Ei to total ET are 68.2 %, 23.6 %, and 8.2 %, respectively, at the Three Rivers Source of the TP (Zhuang et al., 2024). Our study suggests that soil evaporation is the largest contributor to total ET in the whole TP, and further study should be given more attention in further studies. We also found that the evaluation of different ET components is still limited due to the scarcity of available data, and comprehensive evaluations based on more observations would help to further evaluate the ET components and improve the algorithm performance.

This discrepancy in the ET partitioning across different datasets cannot be explained by a single factor, and it is difficult to say which one plays a dominant role as they all contribute in some way to the uncertainty in modelling ET, and may even compensate for each other. In general, these differences stem from factors such as differences in the forcing data, model structure and parameterization, spatial and temporal resolution of the products, and the assumptions embedded in each dataset.

Differences in the forcing data. The forcing data could lead to differences in both the total ET and its components. This explains why GLEAMv35a and GLEAMv35b showed different ET partitioning results, although they are based on exactly the same algorithm. ETMonitor uses GLASS-MODIS data (LAI, FVC, and albedo), PMLV2 use the official MODIS dataset (LAI, albedo, and emissivity). A study by Li et al. (2018) has shown that GLASS LAI is more accurate than MODIS LAI, and MODIS LAI is much lower than GLASS LAI in the eastern TP, which partly explains the relatively lower Ec values by PMLV2 than ETMonitor. Moreover, they also use different meteorological datasets. GLDAS-CLSM uses ERA5 data, while GLDAS-Noah and GLDAS-VIC use GLDAS-2.1 meteorological forcing data as input. A recent study shows that GLDAS-2.1 highly overestimates relative humidity during spring and winter time (Xu et al., 2024), which may lead to lower Es.

Model structure and parameterization. As a most intuitive example, GLDAS-VIC and GLDAS-Noah share the same forcing data, but the estimated ET partitioning differs significantly. GLDAS-VIC gives a much higher Ec/ET and lower Es/ET, consistent with previous studies. This is most likely due to the weaker soil moisture-ET coupling in the applied physical scheme (Feng et al., 2023). The extremely high Ec/ET ratio is mainly due to the "big leaf" vegetation scheme, which assumes that there are no canopy gaps or exposed soil between plants, so that soil evaporation only occurs in unvegetated areas (Bohn and Vivoni, 2016; Sun et al., 2021). It has also been reported that VIC model, with FVC set to 1 as default value, significantly overestimate Ec and suppresses Es in sparse vegetation types with a true FVC between 0.1 and 0.5 (Schaperow et al., 2021). In contrast, GLDAS-CLSM tends to underestimate the Ec/ET ratio and overestimate Es/ET, possibly due to parameterization issues related to the soil or vegetation resistance, or the non-traditional approach of accounting for subgrid heterogeneity in soil moisture (Feng et al., 2023; Sun et al., 2023). CLSM estimates of ET are adjusted by varying the sub-ranges of soil water availability, i.e. the saturation, transpiration and wilting sub-ranges (where transpiration is shut off), which differs from the continuous soil water stress function used in other models. Some other factors, such as the absence of irrigation and the data assimilation procedure, could also affect the ET partitioning in GLDAS models (Li et al., 2022).

Calibration of model parameter. Some ET algorithms may have been calibrated and evaluated against different observations, which can lead to variations in the model performance and, consequently, the partitioning of ET. The global ET datasets use default parameters assigned according to land surface characteristics, which are inappropriate for TP and certainly contribute to differences in ET partitioning. Many studies have also highlighted the importance of parameter optimization to reflect the local vegetation and soil properties for modelling ET processes (Xu et al., 2019; Zheng et al., 2022).

Effects of spatial heterogeneity and resolution. Higher spatial resolution data may more accurately capture details of the local variability in land surface characteristics and associated vapour fluxes in heterogeneous areas (Chen et al., 2019), leading to differences in ET estimates compared to coarser resolution datasets.

4.4 Water vapor released by ~~Tibetan Plateau~~the TP

4.~~3~~4.1 ET magnitude and ~~variation~~variability in the TP

This study confirms the large discrepancy in ~~ET~~the magnitude of ET among ~~various~~different products, as previously reported ~~in studies~~ (e.g., Wang et al., 2020; W. Wang et al., 2018; X. Li et al., 2019). It also ~~reveals substantial deviations~~shows significant differences in ~~terms of~~the spatiotemporal distribution of ET and ET components ~~by~~according to different products. Our study suggests that the ET ~~across~~over the TP ranges from ~~224mm~~224 mm/yr to ~~519mm~~519 mm/yr depending on the products used, with ~~an average~~a mean (median) value of ~~350.34 (362.21~~333.1 (339.8) mm/yr and a standard deviation of 42.~~46~~5 mm/yr. ET accounts for ~~roughly 55~~about 52% of the total annual ~~total~~ precipitation. This study ~~mainly focuses~~focused on the vapor released into the atmosphere, while the downward vapor flux (mainly condensation) ~~is~~was not considered. A recent study based on ERA5 reanalysis data found that the annual mean condensation in the TP is ~~approximately~~about 8.45 mm/yr, which accounts for roughly 2% of the upward vapor flux (Li et al., 2022).~~2022). The surface condensation is generally rare in glacier due to the continuous low temperature on the glacier surface (≤0°C), and therefore can be ignored in statistics (Guo et al., 2022).~~ We also noticed that the boundary of the TP used in this study differs from that ~~of~~used in some previous studies (e.g., Wang et al., 2020; Ma et al., 2021). The boundary we adopted is more reliable ~~as~~because it is based on geomorphology and

带格式的: 字体颜色: 自动设置

带格式的: 字体颜色: 自动设置

带格式的: 字体颜色: 自动设置

带格式的: 字体颜色: 自动设置

带格式的: 字体颜色: 自动设置

formation processes that considerstake into account factors such as elevation, hydrological watershed, etetc., which we believe is more completed and suitableappropriate for land surface processthe analysis of land surface processes (Zhang et al., 2013; Zhang et al., 2021).

Due to the heterogeneity of the climate and land surface, the dominant processes vary acrossbetween the different sub-regions of the TP. For example, plant transpiration is expected to be the dominant process in the humid plant-soil systems whichthat are more abundantcommon in the eastern and southeastern TP, whilewhereas soil evaporation is expected to be the dominant process in the middlecentral to western TP where arid sparse-vegetated or bare soil cover is prevalent. The difference between these processes surely impacted bothcertainly affects the magnitude of ET magnitudes and the responses to the governing factors.. In the eastern and southeastern TP where ET is higher due to the wethumid climate and high vegetation coverscover, there are strong correlations between Rn and ET indicating that biologicalthe water and carbon cycles play an important role, and plant leafthat the stomatal openness and closure of plant leaves are closely related to the radiation forceforcing. In contrast, in the middlecentral and western TP, we foundthere are high correlations between precipitation and ET in the middle and western TP due to the cold arid climate and sparse vegetation covers, and thecover, i.e. abiotic processes are more dominant. Meanwhile, we should notice that these factors are not fully independent. Plants tend to grow more (high LAI) in regions where water is abundant, while higher LAI leads to higher Rn due to the generally low albedo of plantvegetation compared to soil. This may be more important in the energy-limited regions of the southeastern TP.

4.34.2 Impact of cryosphere on surface water flux

Cryosphere element The dynamics of cryosphere elements, such as glacierglaciers and snow, affect water fluxhave a significant impact on hydrological processes significantly. The snow. Snow/ice sublimation constitutes asis one of the most important aspects of water resources and hydrology in the higher at high altitude (MacDonald et al., 2010). Sublimation contributes significantlyis a major contributor to the decrease in snow cover fraction during winter, especially in areas with thin snow cover, and more than half of the snow mass was lost by sublimation during winter in TP (Ueno et al., 2007; Qin et al., 2006).. This study found that snow/ice sublimation (water phase change directly from solid to vapor) in the TP is roughly 14mmabout 14 mm/yr (median value of different productproducts). It may lead to 4% ofan error of 4% if sublimation is not countedtaken into account when estimating the total watervapour flux released byfrom the TP to the atmosphere. The sublimation Sublimation from snow and ice surfaces occurs primarilymainly at high elevations when snow/ice covers large portionsparts of the catchmentcatchments and atmospheric conditions are cold and dry. The , as dictated by the Clausius-Clapeyron equation. The maximum sublimation value is higher than 100mm100 mm/yr in TP (Figure 12). A recent observationsobservational study of the Langtang Valley in the Centralcentral Himalaya inof Nepal showsshowed that the snow sublimation consumes more energy than evaporation, and the snow sublimation iswas 32~74 mm/yr during 2017~2019 (Stigter et al., 2021), which is consistent with the ETMonitor estimation by ETMonitor (48 mm/yr) (Zheng et al.., 2022). Meanwhile, the melting of glaciers replenishes the downstream soil water and lead an increasing of Meltwater from glaciers is a significant proportion of the water available

带格式的: 字体颜色: 自动设置

带格式的: 字体颜色: 自动设置

带格式的: 字体颜色: 自动设置

带格式的: 字体颜色: 自动设置

带格式的: 字体颜色: 自动设置

带格式的: 字体颜色: 自动设置

downstream, which will also enhance theincreases ET process. A study has reported contrasting tendenciestrends in ET in the central TP between a wetland replenished by glaciers melting waterglacial meltwater and thea nearby alpine steppe without the impact of glaciers in central TPwith water supply by precipitation only (Ma et al., 2021).

带格式的: 字体颜色: 自动设置

5. ConclusionConclusions

带格式的: 字体颜色: 自动设置

带格式的: 字体颜色: 自动设置

To clarify the magnitude and variability of water vapour released to the atmosphere in the TP, this study evaluated the performance off 22 ET products in Tibetan Plateau the TP in terms of accuracy, spatial variation,and temporal variation, variability and ET components, response to environmental factors.. The accuracy of the ET products is validated by comparing withwas evaluated against either ground flux towereddy covariance observations or basin-scale estimates of the water balance estimations. The spatiotemporal variationsvariability of ET and its components were intercompared, and the response of ET in TP to precipitation, net surface radiation and leaf area index was explored based on the Pearson correlation analysis. Followingwas evaluated. The main conclusions were obtained:

- According to our validation, the remote sensingThe high-resolution remote sensing-based ET data from ETMonitor and PMLV2 generally showed comparable high accuracy asa comparable to the regional MOD16STMMOD16-STM ET product, with overall better accuracy than other global ET data with fine spatial resolution (~1km).) global ET data. The accuracy of these ET estimates was confirmed by the comparison with the water balance-based ET at basin scale, which further indicated overall accuracy of GLEAM and TerraClimate for the coarse-resolution ET products.
- The median and mean values of annual ET in the TP, according to the multipledifferent products evaluated in this study, are 362.21339.8 mm/yr and 350.34333.1 mm/yr respectively, with a standard deviation of 42.4638.3 mm/yr. Different products showed different spatial and temporal patterns, and large deviations occurred in the middlecentral and western TP. Most products presentedshowed an increasing trend of annual ET in the TP from 2000 to 2020, andwith the annual rate varies depending on thevarying between data products.
- The separate contributions of the different components, i.e. plant transpiration, soil evaporation, interception loss, open water evaporation, and snow/ice sublimation, vary substantially considerably between data products, even in cases in whichwhere total ET agrees wellis in good agreement between the different products, and soil evaporation accounts for mostthe majority of ET. The contributions of open water evaporation and snow/ice sublimation are also not negligible.
- ET is regulated by precipitation, net radiation, and LAI. The effect of precipitation on ET is clearly illustrated, especially in the middle and northern TP. The net radiation plays significant role in the eastern TP, while a high correlation between ET and LAI was also found occasionally in the TP.

Acknowledgements:

This work is funded by the Second Tibetan Plateau Scientific Expedition and Research Program (Grant ~~no~~No. 2019QZKK0206, ~~2019QZKK0103082~~2019QZKK0103) and National Natural Science Foundation of China (Grant ~~no. 42090014,~~No. 42171039). This work is also supported by the International Fellowship Initiative of CEOP – AEGIS and CSC Fellowship. MM acknowledges the MOST High Level Foreign Expert program (Grant No. G2022055010L) and the Chinese Academy of Sciences President's International Fellowship Initiative (Grant No. 2020VTA0001).

Author Contributions:

Dr. C. Zheng: Conceptualization, Methodology, Software, Validation, Formal analysis, Investigation, Resources, Data curation, Writing - original draft, Visualization. Prof. L. Jia: Conceptualization, Methodology, Resources, Data curation, Writing - review & editing, Supervision, Project administration, Funding acquisition. Dr. G Hu: Methodology, Validation, Writing - review & editing. Prof. M. Menenti: ~~Writing~~Conceptualization, writing - review & editing. Dr. J. Timmermans: Writing - review & editing.

Data availability:

The data in study are all from open accessed datasets. FLUXNET data is available from data portal of fluxnet (https://fluxnet.org/). The ChinaFLUX data is available from the data portal of National Ecosystem Research Network of China (http://www.cnern.org.cn/). TORP data and TPHiPr precipitation data is available from National Tibetan Plateau Data Center (http://data.tpdc.ac.cn/). GLASS datasets are available from the University of Maryland (http://glass.umd.edu/). MERRA2 and GLDAS data are available from the Goddard Earth Sciences Data and Information Services Center (https://disc.gsfc.nasa.gov/). The MODIS datasets are available from NASA Earthdata Search (https://search.earthdata.nasa.gov/). The ETMonitor ET is available from CASEARTH Data Sharing and Service Portal (https://data.casearth.cn/). The GLEAM product is available from its official site (www.gleam.eu). The MOD16-STM, EB ET, CR, PMLV2 and PMLV2-Tibet ET datasets are available from TPDC (https://data.tpdc.ac.cn/). The FLUXCOM ET dataset is available from its official website (www.fluxcom.org). The ERA5 and ERA5-Land datasets are available from the Copernicus Climate Data Store (https://cds.climate.copernicus.eu/). SSEBop is available from USGS (https://earlywarning.usgs.gov/ssebop/). TerraClimate is available from Climatology Lab (https://www.climatologylab.org/). SynthesisET is available from the Harvard Data public repository (https://doi.org/10.7910/DVN/ZGOUED). BESSv2 is available from the Seoul National University (https://www.environment.snu.ac.kr/bessv2).

带格式的: 字体颜色: 自动设置
带格式的: 字体颜色: 自动设置
带格式的
带格式的: 字体颜色: 自动设置
带格式的: 字体颜色: 自动设置
带格式的
带格式的
带格式的
带格式的
带格式的
带格式的
带格式的
带格式的
带格式的
带格式的
带格式的
带格式的
带格式的
带格式的
带格式的

Conflicts of Interest:

The authors declare that they have no conflict of interest.

References

Abatzoglou, J. T., Dobrowski, S. Z., Parks, S. A., and Hegewisch, K. C.: TerraClimate, a high-resolution global dataset of monthly climate and climatic water balance from 1958-2015, Sci. Data, 5, https://doi.org/10.1038/sdata.2017.191, 2018.

Baldocchi, D. D.: How eddy covariance flux measurements have contributed to our understanding of Global Change Biology, https://doi.org/10.1111/gcb.14807, 2020.

Bibi, S., Wang, L., Li, X., Zhou, J., Chen, D., and Yao, T.: Climatic and associated cryospheric, biospheric, and hydrological changes on the Tibetan Plateau: a review, https://doi.org/10.1002/joc.5411, 2018.

Bohn, T.J., Vivoni, E.R.: Process-based characterization of evapotranspiration sources over the north american monsoon region. Water Resour. Res., 52 (1), 358–384, https://doi.org/10.1002/2015WR017934. 2016.

Chang, Y., Qin, D., Ding, Y., Zhao, Q., and Zhang, S.: A modified MOD16 algorithm to estimate evapotranspiration over alpine meadow on the Tibetan Plateau, China, J. Hydrol., 561, 16–30, https://doi.org/10.1016/j.jhydrol.2018.03.054, 2018.

Chen, Y., Xia, J., Liang, S., Feng, J., Fisher, J. B., Li, X., Li, X., Liu, S., Ma, Z., Miyata, A., Mu, Q., Sun, L., Tang, J., Wang, K., Wen, J., Xue, Y., Yu, G., Zha, T., Zhang, L., Zhang, Q., Zhao, T., Zhao, L., and Yuan, W.: Comparison of satellite-based evapotranspiration models over terrestrial ecosystems in China, Remote Sens. Environ., 140, 279–293, https://doi.org/10.1016/j.rse.2013.08.045, 2014.

Chen, D., Xu, B., Yao, T., Guo, Z., Cui, P., Chen, F., Zhang, R., Zhang, X., Zhang, Y., Fan, J., Hou, Z., and Zhang, T.: Assessment of past, present and future environmental changes on the Tibetan Plateau, Chinese Sci. Bull., 60, https://doi.org/10.1360/N972014-01370, 2015.

Chen, J., Tan, H., Ji, Y., Tang, Q., Yan, L., Chen, Q., and Tan, D.: Evapotranspiration components dynamic of highland barley using PML ET product in Tibet, Remote Sens., 13, https://doi.org/10.3390/rs13234884, 2021.

Chen, J. M. and Liu, J.: Evolution of evapotranspiration models using thermal and shortwave remote sensing data, Remote Sens. Environ., 237, 111594, https://doi.org/10.1016/j.rse.2019.111594, 2020.

Chen, Q., Jia, L., Menenti, M., Hutjes, R., Hu, G., Zheng, C., and Wang, K.: A numerical analysis of aggregation error in evapotranspiration estimates due to heterogeneity of soil moisture and leaf area index, Agric. For. Meteorol., 269–270, 335–350, https://doi.org/10.1016/j.agrformet.2019.02.017, 2019.

Chen, X., Su, Z., Ma, Y., Trigo, I., and Gentine, P.: Remote Sensing of Global Daily Evapotranspiration based on a Surface Energy Balance Method and Reanalysis Data, J. Geophys. Res. Atmos., 126, 1–22, https://doi.org/10.1029/2020JD032873, 2021.

Chen, X. Yuan, L., Ma, Y., Chen, D., Su, Z., Cao., D.: A doubled increasing trend of evapotranspiration on the Tibetan Plateau.

Sci. Bull., https://doi.org/10.1016/j.scib.2024.03.046, 2024.

Crago, R. D., Szilagyi, J., and Qualls, R.: Comment on: "a review of the complementary principle of evaporation: From the original linear relationship to generalized nonlinear functions" by Han and Tian (2020), Hydrol. Earth Syst. Sci., 25, https://doi.org/10.5194/hess-25-63-2021, 2021.

Cui, J., Tian, L., Wei, Z., Huntingford, C., Wang, P., Cai, Z., Ma, N., and Wang, L.: Quantifying the Controls on Evapotranspiration Partitioning in the Highest Alpine Meadow Ecosystem, Water Resour. Res., 56, https://doi.org/10.1029/2019WR024815, 2020.

Elnashar, A., Wang, L., Wu, B., Zhu, W., and Zeng, H.: Synthesis of global actual evapotranspiration from 1982 to 2019, Earth Syst. Sci. Data, 13, 447–480, https://doi.org/10.5194/essd-13-447-2021, 2021.

Feng, Y.,·Du, S.,·Fraedrich, K., ·Zhang, X., ·Du, M., ·Cheng, W.: Local climate regionalization of the Tibetan Plateau: A data-driven scale-dependent analysis. Theor. Appl. Climatol., https://doi.org/10.1007/s00704-024-04916-8, 2024.

Foken, T.: The energy balance closure problem: An overview, Ecol. Appl., 18, https://doi.org/10.1890/06-0922.1, 2008.

Gelaro, R., McCarty, W., Suárez, M. J., Todling, R., Molod, A., Takacs, L., Randles, C. A., Darmenov, A., Bosilovich, M. G., Reichle, R., Wargan, K., Coy, L., Cullather, R., Draper, C., Akella, S., Buchard, V., Conaty, A., da Silva, A. M., Gu, W., Kim, G. K., Koster, R., Lucchesi, R., Merkova, D., Nielsen, J. E., Partyka, G., Pawson, S., Putman, W., Rienecker, M., Schubert, S. D., Sienkiewicz, M., and Zhao, B.: The modern-era retrospective analysis for research and applications, version 2 (MERRA-2), J. Clim., 30, https://doi.org/10.1175/JCLI-D-16-0758.1, 2017.

Gupta, H. V., Kling, H., Yilmaz, K. K., and Martinez, G. F.: Decomposition of the mean squared error and NSE performance criteria: Implications for improving hydrological modelling, J. Hydrol., 377, https://doi.org/10.1016/j.jhydrol.2009.08.003, 2009.

Han, S. and Tian, F.: A review of the complementary principle of evaporation: From the original linear relationship to generalized nonlinear functions, https://doi.org/10.5194/hess-24-2269-2020, 2020.

He, J., Yang, K., Tang, W., Lu, H., Qin, J., Chen, Y., and Li, X.: The first high-resolution meteorological forcing dataset for land process studies over China, Sci. Data, 7, https://doi.org/10.1038/s41597-020-0369-y, 2020.

Hersbach, H., Bell, B., Berrisford, P., Hirahara, S., Horányi, A., Muñoz-Sabater, J., Nicolas, J., Peubey, C., Radu, R., Schepers, D., Simmons, A., Soci, C., Abdalla, S., Abellan, X., Balsamo, G., Bechtold, P., Biavati, G., Bidlot, J., Bonavita, M., De Chiara, G., Dahlgren, P., Dee, D., Diamantakis, M., Dragani, R., Flemming, J., Forbes, R., Fuentes, M., Geer, A., Haimberger, L., Healy, S., Hogan, R. J., Hólm, E., Janisková, M., Keeley, S., Laloyaux, P., Lopez, P., Lupu, C., Radnoti, G., de Rosnay, P., Rozum, I., Vamborg, F., Villaume, S., and Thépaut, J. N.: The ERA5 global reanalysis, Q. J. R. Meteorol. Soc., 146, https://doi.org/10.1002/qj.3803, 2020.

Feng, H., Wu, Z., Dong, J., Zhou, J., Brocca, L., He, H.: Transpiration – Soil evaporation partitioning determines inter-model differences in soil moisture and evapotranspiration coupling. Remote Sensing of Environment, 298, https://doi.org/10.1016/j.rse.2023.113841, 2023.

Hu, Z., Yu, G., Zhou, Y., Sun, X., Li, Y., Shi, P., Wang, Y., Song, X., Zheng, Z., Zhang, L., and Li, S.: Partitioning of evapotranspiration and its controls in four grassland ecosystems: Application of a two-source model, Agric. For. Meteorol., 149, https://doi.org/10.1016/j.agrformet.2009.03.014, 2009.

Immerzeel, W. W., Lutz, A. F., Andrade, M., Bahl, A., Biemans, H., Bolch, T., Hyde, S., Brumby, S., Davies, B. J., Elmore, A. C., Emmer, A., Feng, M., Fernández, A., Haritashya, U., Kargel, J. S., Koppes, M., Kraaijenbrink, P. D. A., Kulkarni, A. V., Mayewski, P. A., Nepal, S., Pacheco, P., Painter, T. H., Pellicciotti, F., Rajaram, H., Rupper, S., Sinisalo, A., Shrestha, A. B., Viviroli, D., Wada, Y., Xiao, C., Yao, T., and Baillie, J. E. M.: Importance and vulnerability of the world's water towers, Nature, 577, https://doi.org/10.1038/s41586-019-1822-y, 2020.

Jia L., Zheng C., Hu G.C., Menenti M.: 4.03 - Evapotranspiration, In Comprehensive Remote Sensing, edited by Shunlin Liang, Elsevier, Oxford. http://10.1016/B978-0-12-409548-9.10353-7, 2018.

Jia, A., Jiang, B., Liang, S., Zhang, X., and Ma, H.: Validation and spatiotemporal analysis of CERES surface net radiation product, Remote Sens., 8, https://doi.org/10.3390/rs8020090, 2016.

Jiang, Y., Yang, K., Qi, Y., Zhou, X., He, J., Lu, H., Li, X., Chen, Y., Li, X., Zhou, B., Mamtimin, A., Shao, C., Ma, X., Tian, J., and Zhou, J.: TPHiPr: a long-term (1979-2020) high-accuracy precipitation dataset (1/30°daily) for the Third Pole region based on high-resolution atmospheric modeling and dense observations, Earth Syst. Sci. Data, 15, https://doi.org/10.5194/essd-15-621-2023, 2023.

Jiang, Y., Tang, R., and Li, Z. L.: A physical full-factorial scheme for gap-filling of eddy covariance measurements of daytime evapotranspiration, Agric. For. Meteorol., 323, https://doi.org/10.1016/j.agrformet.2022.109087, 2022.

Jiao, D., Xu, N., Yang, F., and Xu, K.: Evaluation of spatial-temporal variation performance of ERA5 precipitation data in China, Sci. Rep., 11, https://doi.org/10.1038/s41598-021-97432-y, 2021.

Jung, M., Koirala, S., Weber, U., Ichii, K., Gans, F., Camps-Valls, G., Papale, D., Schwalm, C., Tramontana, G., and Reichstein, M.: The FLUXCOM ensemble of global land-atmosphere energy fluxes, Sci. Data, 6, 1–14, https://doi.org/10.1038/s41597-019-0076-8, 2019.

Kato, T., Tang, Y., Gu, S., Hirota, M., Cui, X., Du, M., Li, Y., Zhao, X., and Oikawa, T.: Seasonal patterns of gross primary production and ecosystem respiration in an alpine meadow ecosystem on the Qinghai-Tibetan Plateau, J. Geophys. Res. D Atmos., 109, https://doi.org/10.1029/2003JD003951, 2004.

Khan, M. S., Baik, J., and Choi, M.: Inter-comparison of evapotranspiration datasets over heterogeneous landscapes across Australia, Adv. Sp. Res., 66, https://doi.org/10.1016/j.asr.2020.04.037, 2020.

Kuang, X. and Jiao, J. J.: Review on climate change on the Tibetan plateau during the last half century, https://doi.org/10.1002/2015JD024728, 2016.

Li, B., Rodell, M., Kumar, S., Beaudoing, H. K., Getirana, A., Zaitchik, B. F., de Goncalves, L. G., Cossetin, C., Bhanja, S., Mukherjee, A., Tian, S., Tangdamrongsub, N., Long, D., Nanteza, J., Lee, J., Policelli, F., Goni, I. B., Daira, D., Bila, M., de Lannoy, G., Mocko, D., Steele-Dunne, S. C., Save, H., and Bettadpur, S.: Global GRACE Data Assimilation for Groundwater and Drought Monitoring: Advances and Challenges, Water Resour. Res., 55, https://doi.org/10.1029/2018WR024618, 2019.

Li, C., Liu, Z., Tu, Z., Shen, J., He, Y., Yang., H.: Assessment of global gridded transpiration products using the extended instrumental variable technique (EIVD). J. Hydrol., 623, https://doi.org/10.1016/j.jhydrol.2023.129880, 2023.

Li, C., Yang, H., Yang, W., Liu, Z., Jia, Y., Li, S., Yang, D.: Error characterization of global land evapotranspiration products: collocation-based approach. J. Hydrol. 612, 128102 https://doi.org/10.1016/j.jhydrol.2022.128102. 2022.

Li, X., Long, D., Han, Z., Scanlon, B. R., Sun, Z., Han, P., and Hou, A.: Evapotranspiration Estimation for Tibetan Plateau Headwaters Using Conjoint Terrestrial and Atmospheric Water Balances and Multisource Remote Sensing, Water Resour. Res., 55, https://doi.org/10.1029/2019WR025196, 2019.

Li, Z., Feng, Q., Li, Z., Yuan, R., Gui, J., and Lv, Y.: Climate background, fact and hydrological effect of multiphase water transformation in cold regions of the Western China: A review, https://doi.org/10.1016/j.earscirev.2018.12.004, 2019.

Li, B., Ryu, Y., Jiang, C., Dechant, B., Liu, J., Yan, Y., and Li, X.: BESSv2.0: A satellite-based and coupled-process model for quantifying long-term global land–atmosphere fluxes, Remote Sens. Environ., 295, https://doi.org/10.1016/j.rse.2023.113696, 2023.

Li, X., Li, X., Li, Z., Ma, M., Wang, J., Xiao, Q., Liu, Q., Che, T., Chen, E., Yan, G., Hu, Z., Zhang, L., Chu, R., Su, P., Liu, Q., Liu, S., Wang, J., Niu, Z., Chen, Y., Jin, R., Wang, W., Ran, Y., Xin, X., and Ren, H.: Watershed allied telemetry experimental research, J. Geophys. Res. Atmos., 114, https://doi.org/10.1029/2008JD011590, 2009.

Li X, Lu H, Yu L, Yang K.: Comparison of the Spatial Characteristics of Four Remotely Sensed Leaf Area Index Products over China: Direct Validation and Relative Uncertainties. Remote Sensing. 10(1),148, https://doi.org/10.3390/rs10010148, 2018.

Liu, S., Li, X., Xu, Z., Che, T., Xiao, Q., Ma, M., Liu, Q., Jin, R., Guo, J., Wang, L., Wang, W., Qi, Y., Li, H., Xu, T., Ran, Y., Hu, X., Shi, S., Zhu, Z., Tan, J., Zhang, Y., and Ren, Z.: The Heihe Integrated Observatory Network: A Basin-Scale Land Surface Processes Observatory in China, Vadose Zo. J., 17, https://doi.org/10.2136/vzj2018.04.0072, 2018.

Liu, H, Xin, X, Su, Z., Zeng, Y., Lian, T., Li, L., Shanshan S.: Hailong Zhang Intercomparison and evaluation of ten global ET products at site and basin scales. J. Hydrol., 617, 128887, https://doi.org/10.1016/j.jhydrol.2022.128887, 2023.

Ma, N., Zhang, Y., Guo, Y., Gao, H., Zhang, H., and Wang, Y.: Environmental and biophysical controls on the evapotranspiration over the highest alpine steppe, J. Hydrol., 529, https://doi.org/10.1016/j.jhydrol.2015.09.013, 2015.

Ma, N., Szilagyi, J., and Zhang, Y.: Calibration-Free Complementary Relationship Estimates Terrestrial Evapotranspiration Globally, Water Resour. Res., 57, 1–27, https://doi.org/10.1029/2021WR029691, 2021.

Ma, N. and Zhang, Y.: Increasing Tibetan Plateau terrestrial evapotranspiration primarily driven by precipitation, Agric. For. Meteorol., 317, https://doi.org/10.1016/j.agrformet.2022.108887, 2022.

Ma, Y., Hu, Z., Xie, Z., Ma, W., Wang, B., Chen, X., Li, M., Zhong, L., Sun, F., Gu, L., Han, C., Zhang, L., Liu, X., Ding, Z., Sun, G., Wang, S., Wang, Y., and Wang, Z.: A long-term (2005–2016) dataset of hourly integrated land–atmosphere interaction observations on the Tibetan Plateau, Earth Syst. Sci. Data, 12, https://doi.org/10.5194/essd-12-2937-2020, 2020.

Ma, Y., Kang, S., Zhu, L., Xu, B., Tian, L., and Yao, T.: Roof of the World: Tibetan observation and research platform, Bull. Am. Meteorol. Soc., 89, https://doi.org/10.1175/2008BAMS2545.1, 2008.

Martens, B., Miralles, D. G., Lievens, H., Van Der Schalie, R., De Jeu, R. A. M., Fernández-Prieto, D., Beck, H. E., Dorigo,

W. A., and Verhoest, N. E. C.: GLEAM v3: Satellite-based land evaporation and root-zone soil moisture, Geosci. Model Dev., 10, 1903–1925, https://doi.org/10.5194/gmd-10-1903-2017, 2017.

Miralles, D. G., Holmes, T. R. H., De Jeu, R. A. M., Gash, J. H., Meesters, A. G. C. A., and Dolman, A. J.: Global land-surface evaporation estimated from satellite-based observations, Hydrol. Earth Syst. Sci., 15, 453–469, https://doi.org/10.5194/hess-15-453-2011, 2011.

Miralles, D. G., Brutsaert, W., Dolman, A. J., and Gash, J. H.: On the Use of the Term "Evapotranspiration," https://doi.org/10.1029/2020WR028055, 2020.

Morton, F. I.: Operational estimates of areal evapotranspiration and their significance to the science and practice of hydrology, J. Hydrol., 66, https://doi.org/10.1016/0022-1694(83)90177-4, 1983.

Mu, Q., Heinsch, F. A., Zhao, M., and Running, S. W.: Mu, Q., Zhao, M., and Running, S. W.: Improvements to a MODIS global terrestrial evapotranspiration algorithm, Remote Sens. Environ., 111, https://doi.org/10.1016/j.rse.2007.04.015, 2007.

Mu, Q., Zhao, M., and Running, S. W.: Improvements to a MODIS global terrestrial evapotranspiration algorithm, Remote Sens. Environ., 115, https://doi.org/10.1016/j.rse.2011.02.019, 2011.

Mueller, B., Hirschi, M., Jimenez, C., Ciais, P., Dirmeyer, P. A., Dolman, A. J., Fisher, J. B., Jung, M., Ludwig, F., Maignan, F., Miralles, D. G., McCabe, M. F., Reichstein, M., Sheffield, J., Wang, K., Wood, E. F., Zhang, Y., and Seneviratne, S. I.: Benchmark products for land evapotranspiration: LandFlux-EVAL multi-data set synthesis, Hydrol. Earth Syst. Sci., 17, 3707–3720, https://doi.org/10.5194/hess-17-3707-2013, 2013.

Muñoz-Sabater, J., Dutra, E., Agustí-Panareda, A., Albergel, C., Arduini, G., Balsamo, G., Boussetta, S., Choulga, M., Harrigan, S., Hersbach, H., Martens, B., Miralles, D. G., Piles, M., Rodríguez-Fernández, N. J., Zsoter, E., Buontempo, C., and Thépaut, J. N.: ERA5-Land: A state-of-the-art global reanalysis dataset for land applications, Earth Syst. Sci. Data, 13, https://doi.org/10.5194/essd-13-4349-2021, 2021.

Rodell, M., Houser, P. R., Jambor, U., Gottschalck, J., Mitchell, K., Meng, C. J., Arsenault, K., Cosgrove, B., Radakovich, J., Bosilovich, M., Entin, J. K., Walker, J. P., Lohmann, D., and Toll, D.: The Global Land Data Assimilation System, Bull. Am. Meteorol. Soc., 85, https://doi.org/10.1175/BAMS-85-3-381, 2004.

Schaperow, J.R., Li, D., Margulis, S.A., Lettenmaier, D.P.: A near-global, high resolution land surface parameter dataset for the variable infiltration capacity model. Sci. Data, 8 (1), 216. https://doi.org/10.1038/s41597-021-00999-4. 2021.

Senay, G. B., Kagone, S., and Velpuri, N. M.: Operational global actual evapotranspiration: Development, evaluation, and dissemination, Sensors (Switzerland), 20, https://doi.org/10.3390/s20071915, 2020.

Shang, L., Zhang, Y., Lü, S., and Wang, S.: Energy exchange of an alpine grassland on the eastern Qinghai-Tibetan Plateau, Sci. Bull., 60, https://doi.org/10.1007/s11434-014-0685-8, 2015.

Shang, K., Yao, Y., Di, Z., Jia, K., Zhang, X., Fisher, J. B., Chen, J., Guo, X., Yang, J., Yu, R., Xie, Z., Liu, L., Ning, J., & Zhang, L.: Coupling physical constraints with machine learning for satellite-derived evapotranspiration of the Tibetan Plateau. Remote Sensing of Environment, 289. https://doi.org/10.1016/j.rse.2023.113519, 2023.

Shen, M., Piao, S., Jeong, S. J., Zhou, L., Zeng, Z., Ciais, P., Chen, D., Huang, M., Jin, C. S., Li, L. Z. X., Li, Y., Myneni, R.

B., Yang, K., Zhang, G., Zhang, Y., and Yao, T.: Evaporative cooling over the Tibetan Plateau induced by vegetation growth, Proc. Natl. Acad. Sci. U. S. A., 112, https://doi.org/10.1073/pnas.1504418112, 2015.

Song, L., Zhuang, Q., Yin, Y., Zhu, X., and Wu, S.: Spatio-temporal dynamics of evapotranspiration on the Tibetan Plateau from 2000 to 2010, Environ. Res. Lett., 12, https://doi.org/10.1088/1748-9326/aa527d, 2017.

Stigter, E. E., Steiner, J. F., Koch, I., Saloranta, T. M., Kirkham, J. D., and Immerzeel, W. W.: Energy and mass balance dynamics of the seasonal snowpack at two high-altitude sites in the Himalaya, Cold Reg. Sci. Technol., 183, https://doi.org/10.1016/j.coldregions.2021.103233, 2021.

Sun, H., Su, F., Yao, T., He, Z., Tang, G., Huang, J., Zheng, B., Meng, F., Ou, T., and Chen, D.: General overestimation of ERA5 precipitation in flow simulations for High Mountain Asia basins, Environ. Res. Commun., 3, https://doi.org/10.1088/2515-7620/ac40f0, 2021.

Sun, J., Yang, K., Yu, Y., Lu, H., and Lin, Y.: Land–Atmosphere Interactions Partially Offset the Accelerated Tibetan Plateau Water Cycle through Dynamical Processes, J. Clim., 36, https://doi.org/10.1175/JCLI-D-22-0686.1, 2023.

Sun, R., Duan Q., Wang, J.: Understanding the spatial patterns of evapotranspiration estimates from land surface models over China. J. Hydrol., 595, 126021, https://doi.org/10.1016/j.jhydrol.2021.126021, 2021.

Twine, T. E., Kustas, W. P., Norman, J. M., Cook, D. R., Houser, P. R., Meyers, T. P., Prueger, J. H., Starks, P. J., and Wesely, M. L.: Correcting eddy-covariance flux underestimates over a grassland, Agric. For. Meteorol., 103, https://doi.org/10.1016/S0168-1923(00)00123-4, 2000.

~~Ueno, K., Tanaka, K., Tsutsui, H., and Li, M.: Snow cover conditions in the Tibetan Plateau observed during the winter of 2003/2004, in: Arctic, Antarctic, and Alpine Research, https://doi.org/10.1657/1523-0430(2007)39[152:SCCITT]2.0.CO;2, 2007.~~

Wang, B., Y. Ma, Z. Su, Y. Wang and W. Ma. Quantifying the evaporation amounts of 75 high-elevation large dimictic lakes on the Tibetan Plateau. Sci. Adv., 6, https://doi.org/10.1126/sciadv.aay8558, 2020.

Wang, L., Han, S., Tian, F., Li, K., Li, Y., Tudaji, M., Cao, X., Nan, Y., Cui, T., Zheng, X., Hu, Z., Wang, W., and Yang, Y. Z.: The Evaporation on the Tibetan Plateau Stops Increasing in the Recent Two Decades, J. Geophys. Res. Atmos., 127, https://doi.org/10.1029/2022JD037377, 2022.

Wang, W., Li, J., Yu, Z., Ding, Y., Xing, W., and Lu, W.: Satellite retrieval of actual evapotranspiration in the Tibetan Plateau: Components partitioning, multidecadal trends and dominated factors identifying, J. Hydrol., 559, https://doi.org/10.1016/j.jhydrol.2018.02.065, 2018.

Wang, Z., Wu, R., and Huang, G.: Low-frequency snow changes over the Tibetan Plateau, Int. J. Climatol., 38, https://doi.org/10.1002/joc.5221, 2018.

Wei, Y., Lu, H., Wang, J., Wang, X., and Sun, J.: Dual Influence of Climate Change and Anthropogenic Activities on the Spatiotemporal Vegetation Dynamics Over the Qinghai-Tibetan Plateau From 1981 to 2015, Earth's Futur., 10, https://doi.org/10.1029/2021EF002566, 2022.

Wu, G., Liu, Y., He, B., Bao, Q., Duan, A., Jin, F.F.: Thermal controls on the Asian summer monsoon. Sci. Rep., 2.

http://dx.doi.org/10.1038/srep00404, 2012.

Wu, G. X., Zhuo, H. F., Wang, Z. Q., and Liu, Y. M.: Two types of summertime heating over the Asian large-scale orography and excitation of potential-vorticity forcing I. Over Tibetan Plateau, Sci. China Earth Sci., 59, https://doi.org/10.1007/s11430-016-5328-2, 2016.

Xiao, Z., Liang, S., Wang, J., Chen, P., Yin, X., Zhang, L., and Song, J.: Use of general regression neural networks for generating the GLASS leaf area index product from time-series MODIS surface reflectance, IEEE Trans. Geosci. Remote Sens., 52, https://doi.org/10.1109/TGRS.2013.2237780, 2014.

Xiao, Z., Song, J., Yang, H., Sun, R., and Li, J.: A 250 m resolution global leaf area index product derived from MODIS surface reflectance data, Int. J. Remote Sens., 43, https://doi.org/10.1080/01431161.2022.2039415, 2022.

Xie, W., Yi, S., Leng, C., Xia, D., Li, M., Zhong, Z., and Ye, J.: The evaluation of IMERG and ERA5-Land daily precipitation over China with considering the influence of gauge data bias, Sci. Rep., 12, https://doi.org/10.1038/s41598-022-12307-0, 2022.

Xu, C., Wang, W., Hu, Y., Liu. Y.: Evaluation of ERA5, ERA5-Land, GLDAS-2.1, and GLEAM potential evapotranspiration data over mainland China. Journal of Hydrology: Regional Studies, 51, https://doi.org/10.1016/j.ejrh.2023.101651, 2024.

Xu, T., Guo, Z., Xia, Y., Ferreira, V.G., Liu, S., Wang, K., Yao, Y., Zhang, X., Zhao, C.: Evaluation of twelve evapotranspiration products from machine learning, remote sensing and land surface models over conterminous United States. J. Hydrol., 578, 124105, https://doi.org/10.1016/j.jhydrol.2019.124105. 2019.

Xue, B. L., Wang, L., Li, X., Yang, K., Chen, D., and Sun, L.: Evaluation of evapotranspiration estimates for two river basins on the Tibetan Plateau by a water balance method, J. Hydrol., 492, 290–297, https://doi.org/10.1016/j.jhydrol.2013.04.005, 2013.

Yang, C., Liu, H., Li, Q., Wang, X., Ma, W., Liu, C., Fang, X., Tang, Y., Shi, T., Wang, Q., Xu, Y., Zhang, J., Li, X., Xu, G., Chen, J., Su, M., Wang, S., Wu, J., Huang, L., Li, X., and Wu, G.: Human expansion into Asian highlands in the 21st Century and its effects, Nat. Commun., 13, https://doi.org/10.1038/s41467-022-32648-8, 2022.

Yang, K., Wu, H., Qin, J., Lin, C., Tang, W., and Chen, Y.: Recent climate changes over the Tibetan Plateau and their impacts on energy and water cycle: A review, Glob. Planet. Change, 112, https://doi.org/10.1016/j.gloplacha.2013.12.001, 2014.

Yang, W., Wang, Y., Liu, X., Zhao, H., Shao, R., and Wang, G.: Evaluation of the rescaled complementary principle in the estimation of evaporation on the Tibetan Plateau, Sci. Total Environ., 699, https://doi.org/10.1016/j.scitotenv.2019.134367, 2020.

Yang, Y., Chen, R., Song, Y., Han, C., Liu, Z., and Liu, J.: Evaluation of five complementary relationship models for estimating actual evapotranspiration during soil freeze-thaw cycles, Hydrol. Res., 52, https://doi.org/10.2166/nh.2021.093, 2021.

Yang, Y., Roderick, M. L., Guo, H., Miralles, D. G., Zhang, L., Fatichi, S., Luo, X., Zhang, Y., McVicar, T. R., Tu, Z., Keenan, T. F., Fisher, J. B., Gan, R., Zhang, X., Piao, S., Zhang, B., and Yang, D.: Evapotranspiration on a greening Earth, https://doi.org/10.1038/s43017-023-00464-3, 2023.

Yao, T., Thompson, L., Yang, W., Yu, W., Gao, Y., Guo, X., Yang, X., Duan, K., Zhao, H., Xu, B., Pu, J., Lu, A., Xiang, Y., Kattel, D. B., and Joswiak, D.: Different glacier status with atmospheric circulations in Tibetan Plateau and surroundings, Nat.

Clim. Chang., 2, https://doi.org/10.1038/nclimate1580, 2012.

Yao, T., Xue, Y., Chen, D., Chen, F., Thompson, L., Cui, P., Koike, T., Lau, W. K. M., Lettenmaier, D., Mosbrugger, V., Zhang, R., Xu, B., Dozier, J., Gillespie, T., Gu, Y., Kang, S., Piao, S., Sugimoto, S., Ueno, K., Wang, L., Wang, W., Zhang, F., Sheng, Y., Guo, W., Ailikun, Yang, X. X., Ma, Y., Shen, S. S. P., Su, Z., Chen, F., Liang, S., Liu, Y., Singh, V. P., Yang, K., Yang, D., Zhao, X., Qian, Y., Zhang, Y., and Li, Q.: Recent third pole's rapid warming accompanies cryospheric melt and water cycle intensification and interactions between monsoon and environment: Multidisciplinary approach with observations, modeling, and analysis, Bull. Am. Meteorol. Soc., 100, https://doi.org/10.1175/BAMS-D-17-0057.1, 2019.

Yao, Y., Liang, S., Li, X., Hong, Y., Fisher, J. B., Zhang, N., Chen, J., Cheng, J., Zhao, S., Zhang, X., Jiang, B., Sun, L., Jia, K., Wang, K., Chen, Y., Mu, Q., and Feng, F.: Bayesian multimodel estimation of global terrestrial latent heat flux from eddy covariance, meteorological, and satellite observations, J. Geophys. Res., 119, https://doi.org/10.1002/2013JD020864, 2014.

Yu, G. R., Wen, X. F., Sun, X. M., Tanner, B. D., Lee, X., and Chen, J. Y.: Overview of ChinaFLUX and evaluation of its eddy covariance measurement, Agric. For. Meteorol., 137, https://doi.org/10.1016/j.agrformet.2006.02.011, 2006.

Yuan, L., Ma, Y., Chen, X., Wang, Y., and Li, Z.: An Enhanced MOD16 Evapotranspiration Model for the Tibetan Plateau During the Unfrozen Season, J. Geophys. Res. Atmos., 126, https://doi.org/10.1029/2020JD032787, 2021.

Yuan, L., Chen, X., Ma, Y., Han, C., Wang, B., and Ma, W.: Long-term monthly 0.05° terrestrial evapotranspiration dataset (1982–2018) for the Tibetan Plateau, Earth Syst. Sci. Data, 16, 775–801. https://doi.org/10.5194/essd-16-775-2024, 2024.

Zhang, G., Yao, T., Xie, H., Kang, S., and Lei, Y.: Increased mass over the Tibetan Plateau: From lakes or glaciers?, Geophys. Res. Lett., 40, https://doi.org/10.1002/grl.50462, 2013.

Zhang, K., Kimball, J. S., Nemani, R. R., and Running, S. W.: A continuous satellite-derived global record of land surface evapotranspiration from 1983 to 2006, Water Resour. Res., 46, https://doi.org/10.1029/2009WR008800, 2010.

Zhang, T., Gebremichael, M., Meng, X., Wen, J., Iqbal, M., Jia, D., et al. Climate-related trends of actual evapotranspiration over the Tibetan Plateau (1961–2010). International Journal of Climatology, 38(S1), e48–e56. https://doi.org/10.1002/joc.5350, 2018.

Zhang, Y., Kong, D., Gan, R., Chiew, F. H. S., McVicar, T. R., Zhang, Q., and Yang, Y.: Coupled estimation of 500 m and 8-day resolution global evapotranspiration and gross primary production in 2002–2017, Remote Sens. Environ., 222, 165–182, https://doi.org/10.1016/j.rse.2018.12.031, 2019.

Zhang, Y., Li, B., Liu, L., Zheng, D: Redetermine the region and boundaries of Tibetan Plateau, Geogr. Res., 40, https://doi.org/10.11821/dlyj020210138, 2021.

Zheng, C., Jia, L., and Hu, G.: Global land surface evapotranspiration monitoring by ETMonitor model driven by multi-source satellite earth observations, J. Hydrol., 613, 128444, https://doi.org/10.1016/j.jhydrol.2022.128444, 2022.

Zheng, C., Jia, L., Hu, G., Lu, J., Wang, K., and Li, Z.: Global Evapotranspiration Derived by ETMonitor Model based on Earth Observations, in: International Geoscience and Remote Sensing Symposium (IGARSS), 222–225, 2016.

Zhou, X., Zhao, P., Chen, J., Chen, L., Li,W.: Impacts of thermodynamic processes over the Tibetan Plateau on the Northern Hemispheric climate. Sci. China Ser. D Earth Sci. 52, 1679–169, https://doi.org/10.1007/s11430-009-0194-9, 2009.

Zhu, W., Wang, Y., and Jia, S.: A remote sensing-based method for daily evapotranspiration mapping and partitioning in a poorly gauged basin with arid ecosystems in the Qinghai-Tibet Plateau, J. Hydrol., 616, https://doi.org/10.1016/j.jhydrol.2022.128807, 2023.

Zhuang, J., Li, Y, Bai, P, Chen, L, Guo, X., Xing, Y., Feng, A, Yu, W., Huang, M.: Changed evapotranspiration and its components induced by greening vegetation in the Three Rivers Source of the Tibetan Plateau. J. Hydrol., 633, 130970, https://doi.org/10.1016/j.jhydrol.2024.130970, 2024.